MRI-driven dynamos in binary neutron star mergers

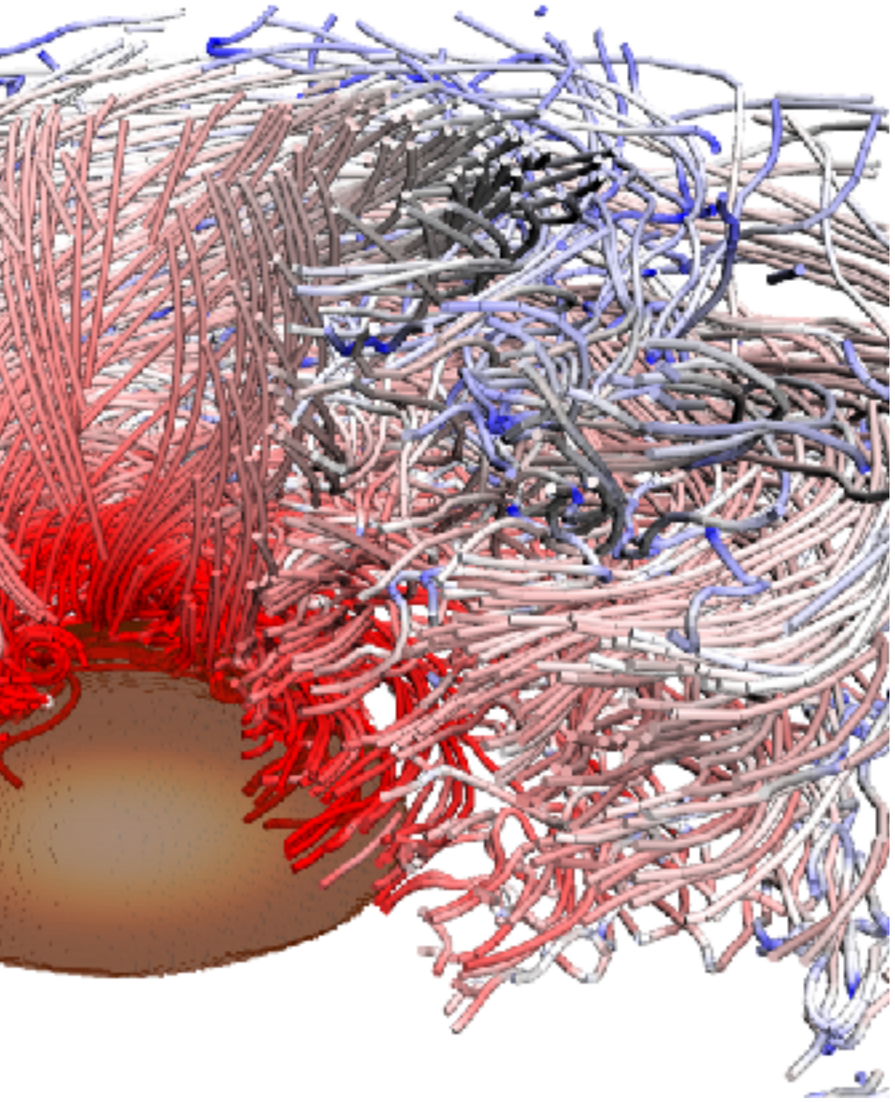

Alexis Reboul-Salze

in collaboration with
Kenta Kiuchi[1], Loren Held[1,2], Masaru Shibata[1],

[1]Max Planck Institute for Gravitational Physics, Potsdam, Germany
[2]DAMTP, Cambridge

Binary neutron star mergers

GW170817 GRB170817A

Nucleosynthesis of heavy elements (r-process)

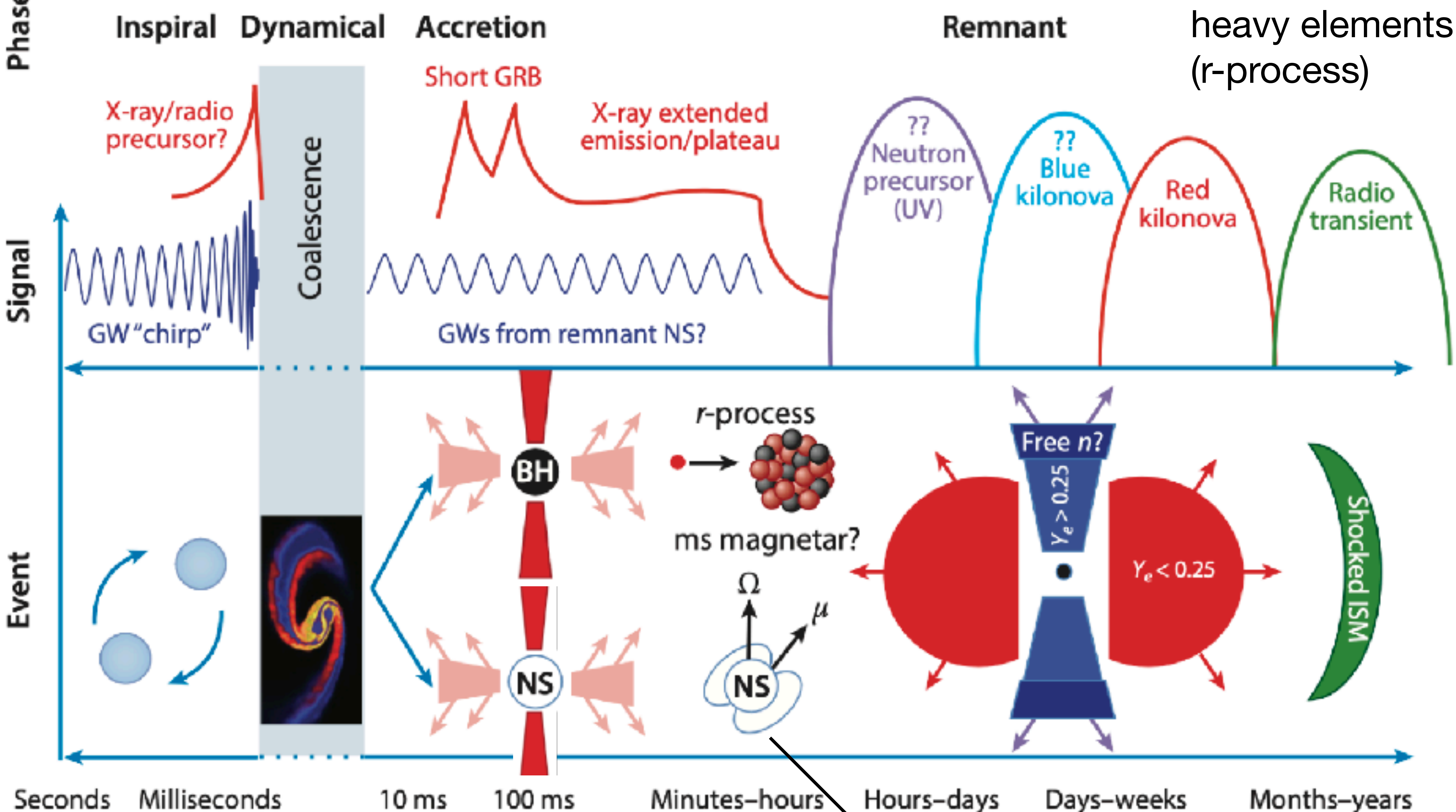

Mode resonances in GW?
See Counsell+2025, Suvorov+ 2024, Kuan+2025, ARS+2025, etc.

Detectability of a magnetar?
See Piasse, ARS et al, soon to be submitted

Fernandez & Metzger 2016

Proto-magnetar central engine with an initial dipole field in the remnant

No-leakage scheme | low resolution | High resolution

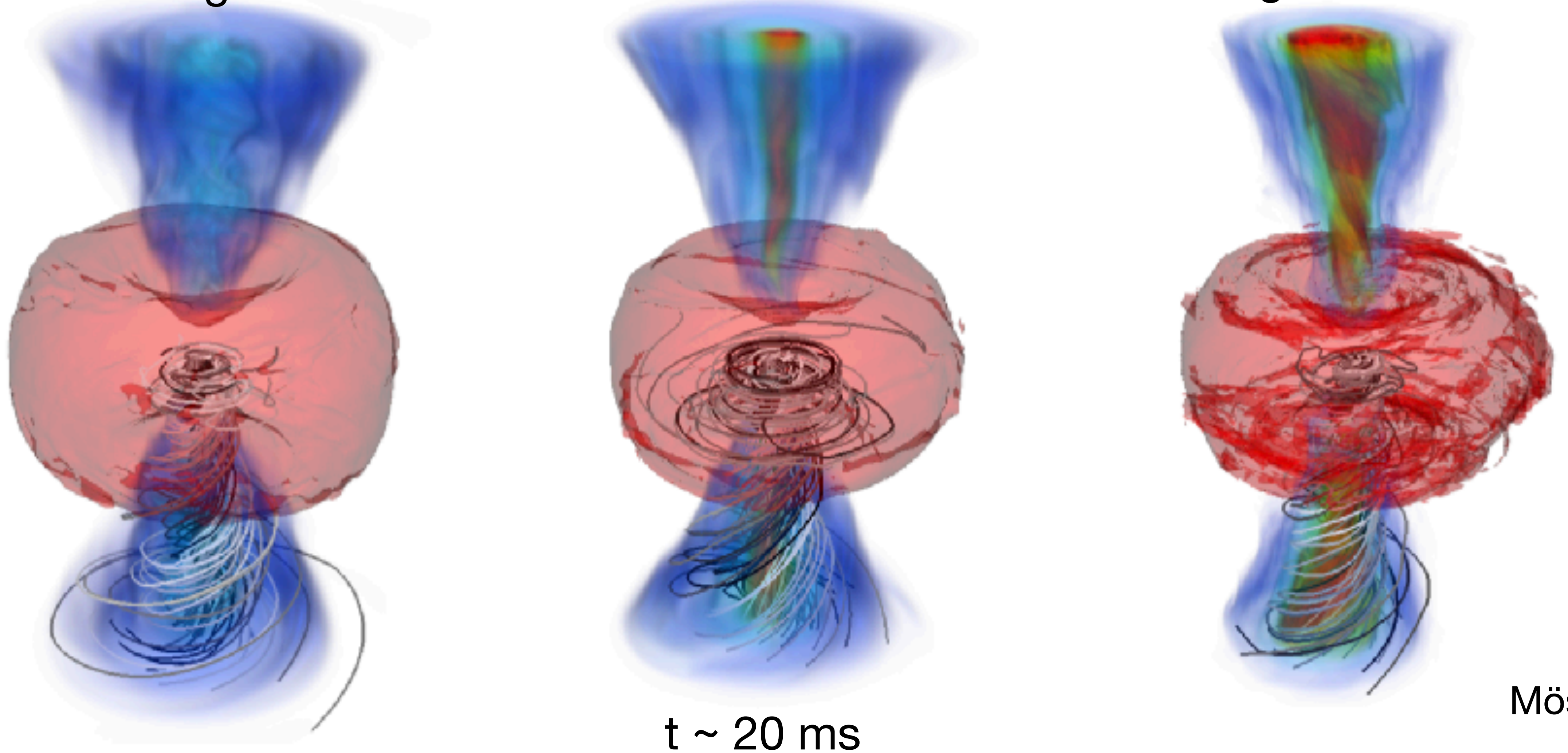

Mösta+2020

t ~ 20 ms

- Initialised with large scale magnetic field of $B \sim 10^{15}$ G
- Extra energy injection → can explain X-ray plateaus in sGRBs but not only explanation

BH + disks and this scenario require a strong large-scale magnetic field

→Three amplification mechanisms in BNS mergers:

Kelvin-Helmholtz instability, **Magnetorotational instability,** **Tayler-Spruit in NS remnant**

Amplification mechanisms in neutron star mergers

Evolution of the merger

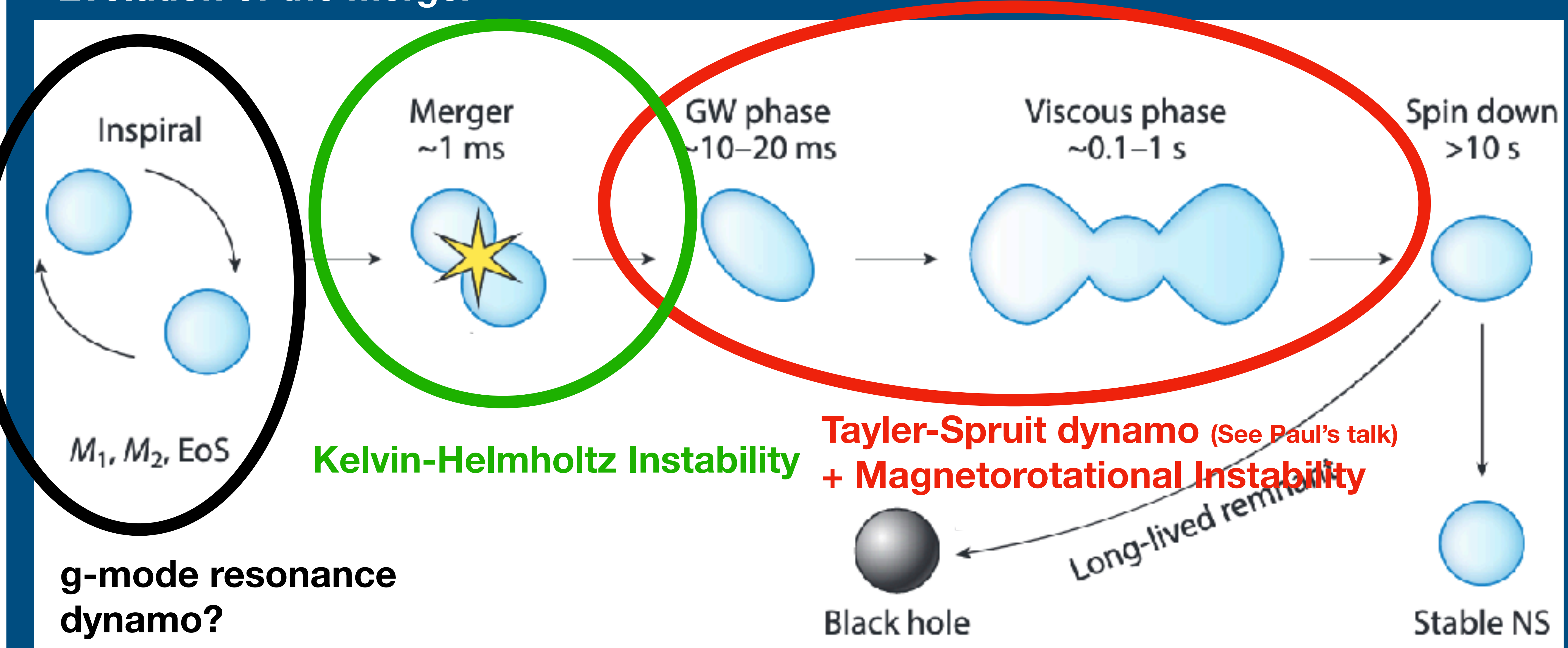

g-mode resonance dynamo?
See ARS+2025c

Radice et al. 2020

Amplification mechanisms in neutron star mergers

Evolution of the merger

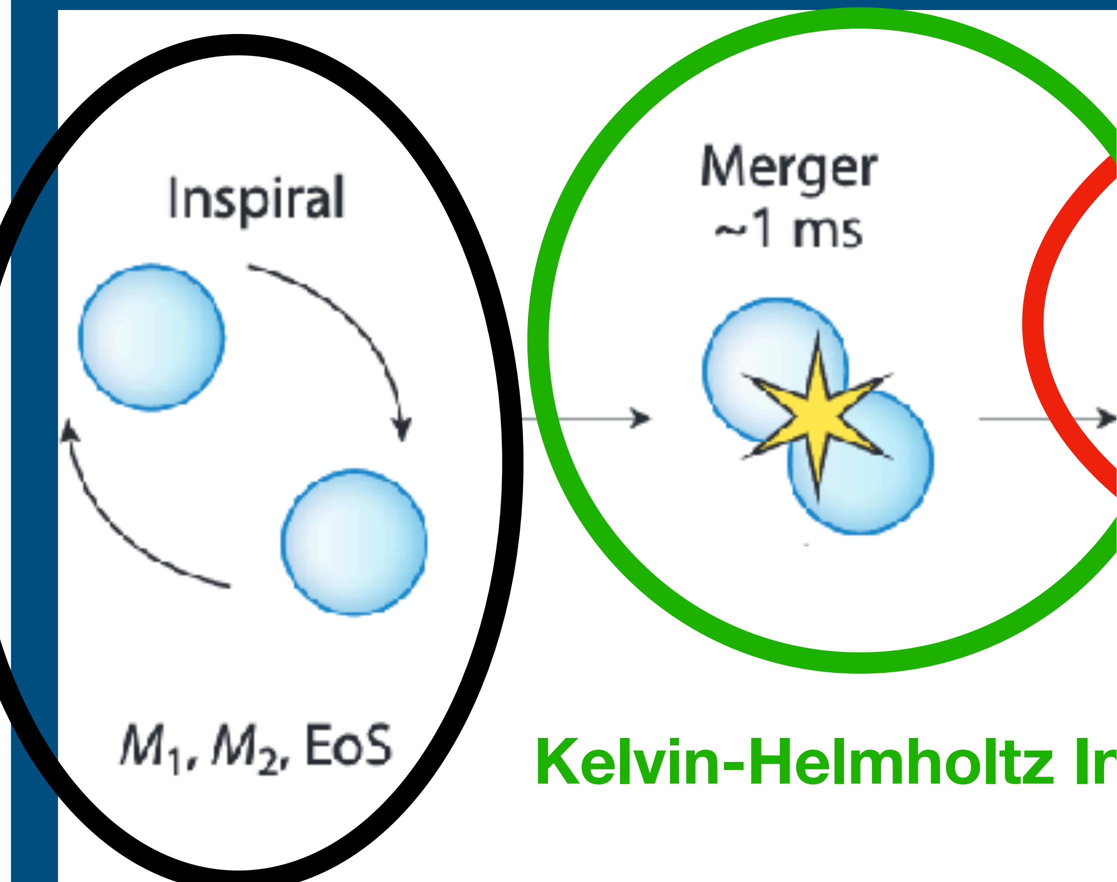

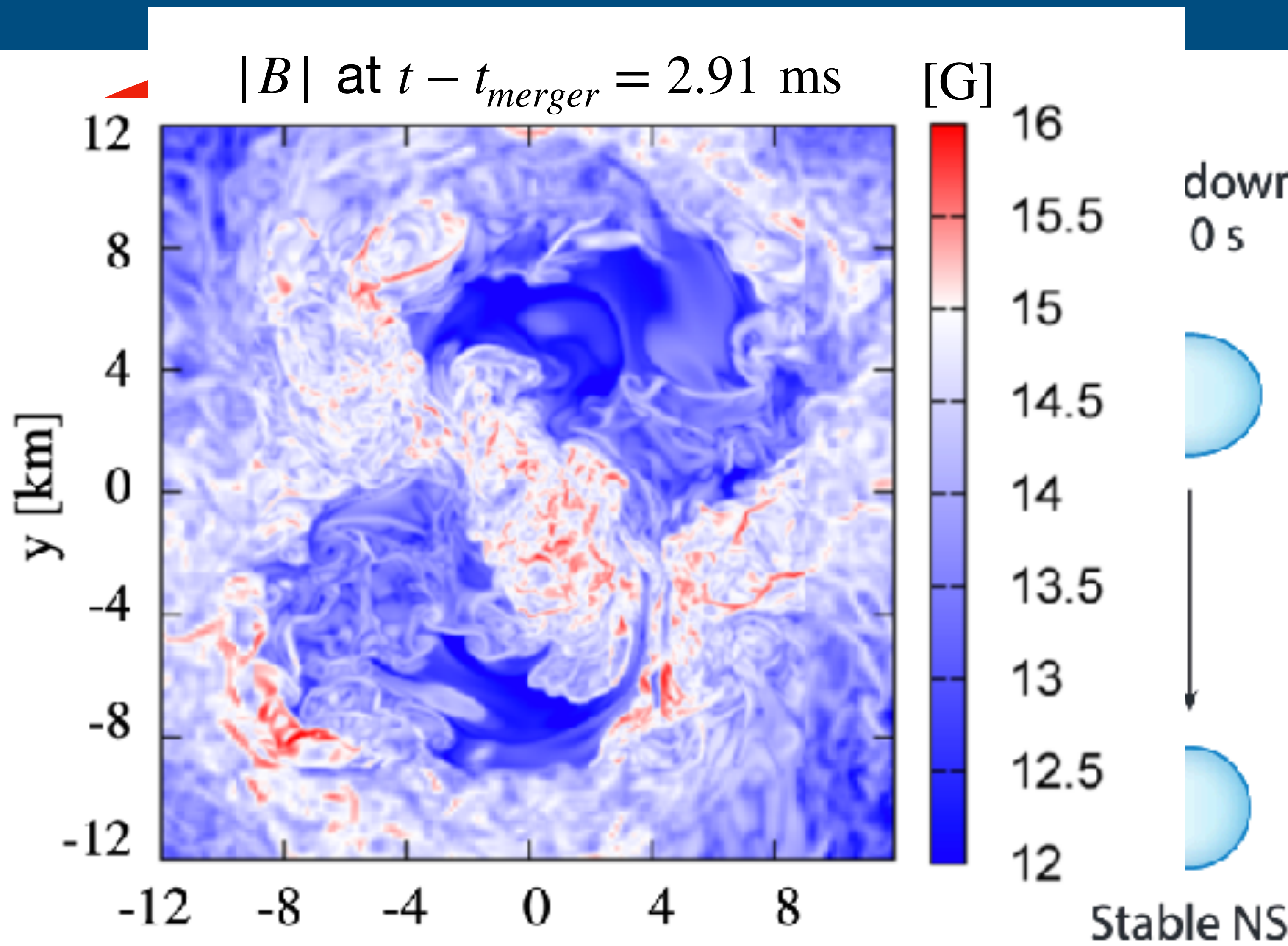

g-mode resonance dynamo?

See ARS+2025c

Kiuchi et al. 2015 . 2020

Amplification from 10^{13} G to 10^{16} G on small scales

Energy saturation at ~a few 10^{50} erg

Initial conditions right after mergers

Converged magnetic field spectrum
at t=10 ms

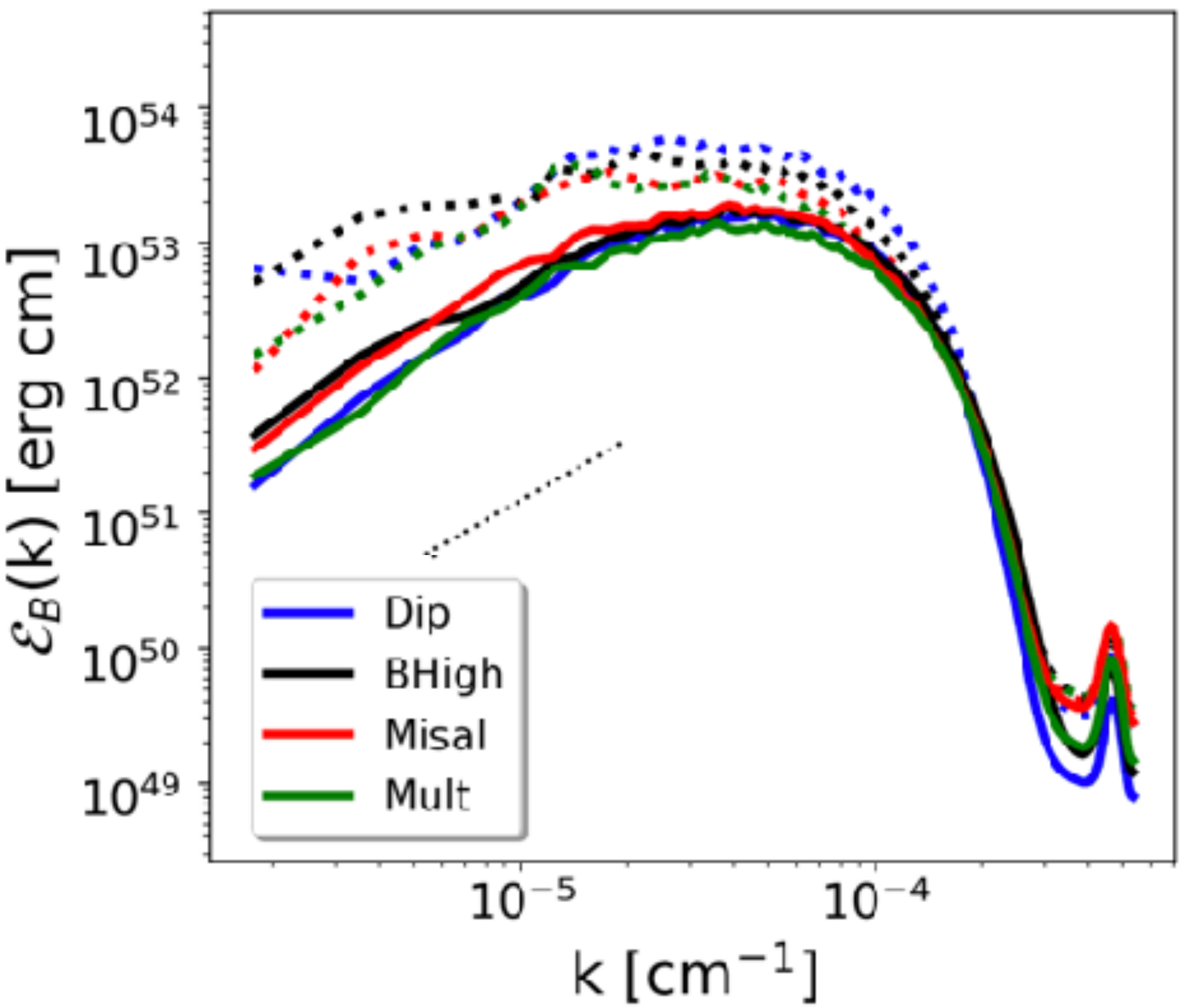

Aguilera-Miret et al. 2022

Tayler-Spruit dynamo?

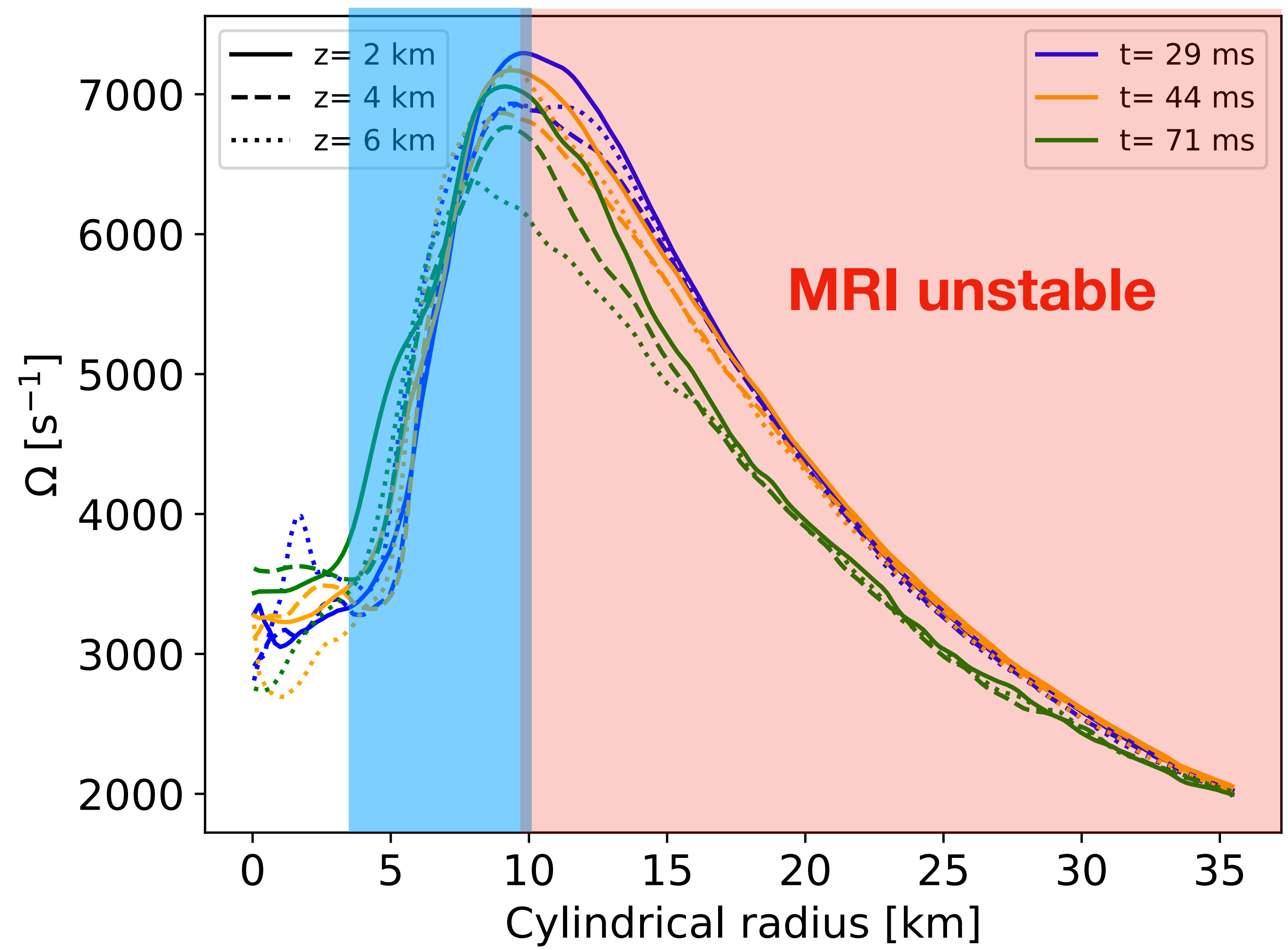

TS dynamo: ARS et al. 2025a

Magneto-rotational instability (MRI)

MRI mechanism in a simple case:

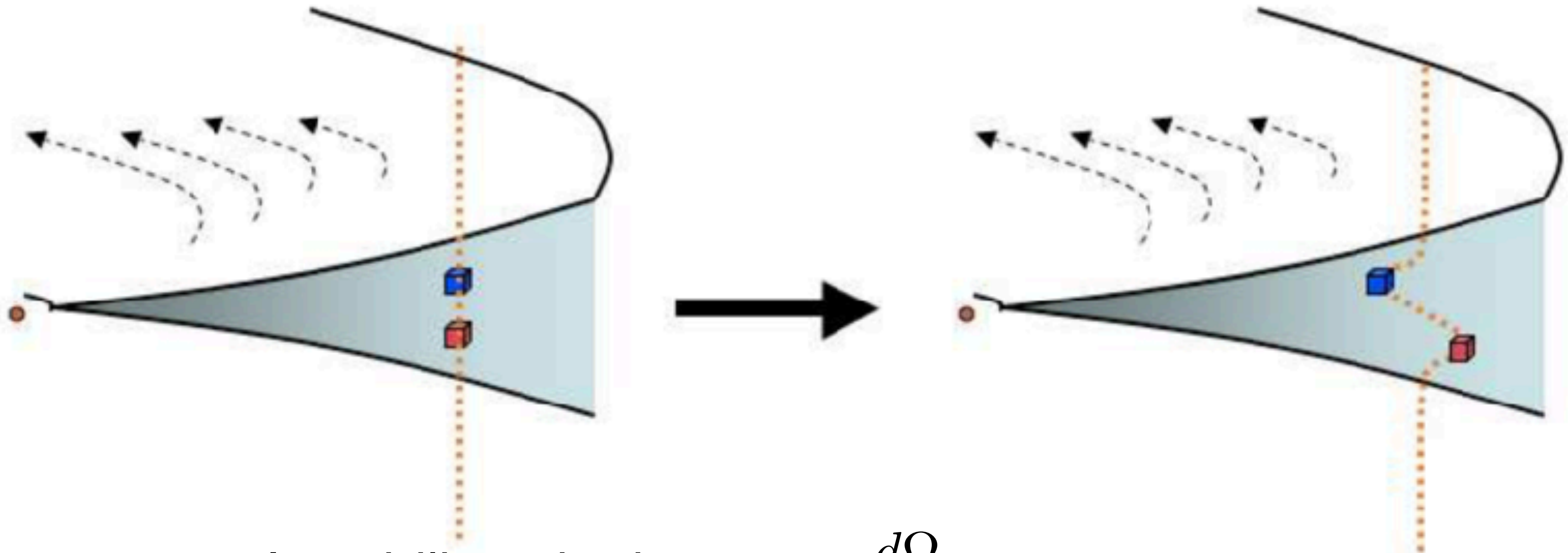

Credit : Fromang

Instability criterion: $\frac{d\Omega}{dr} < 0$

Growth rate: $\sigma = \frac{q\Omega}{2}$ with $\Omega \propto r^{-q}$

→ Fast growth for fast rotation

Wavelength: $\lambda_{MRI} \propto \frac{B}{\sqrt{\rho}\Omega}$

→ Short wavelength for weak magnetic fields

See Jannaud+2025 for derivation in zero-net flux setups

Local models of the MRI

“Shearing box” models

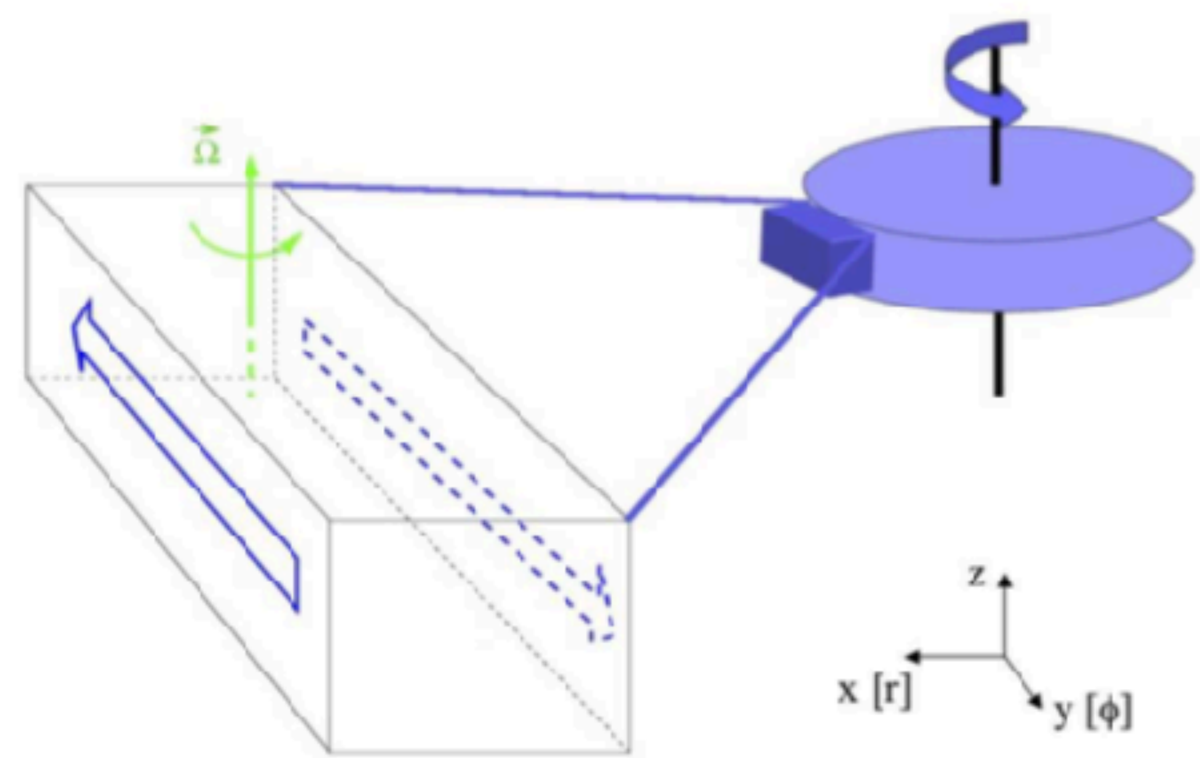

Ideal/non-ideal MHD equations

Credit: G. Lesur

MHD turbulence: toroidal field

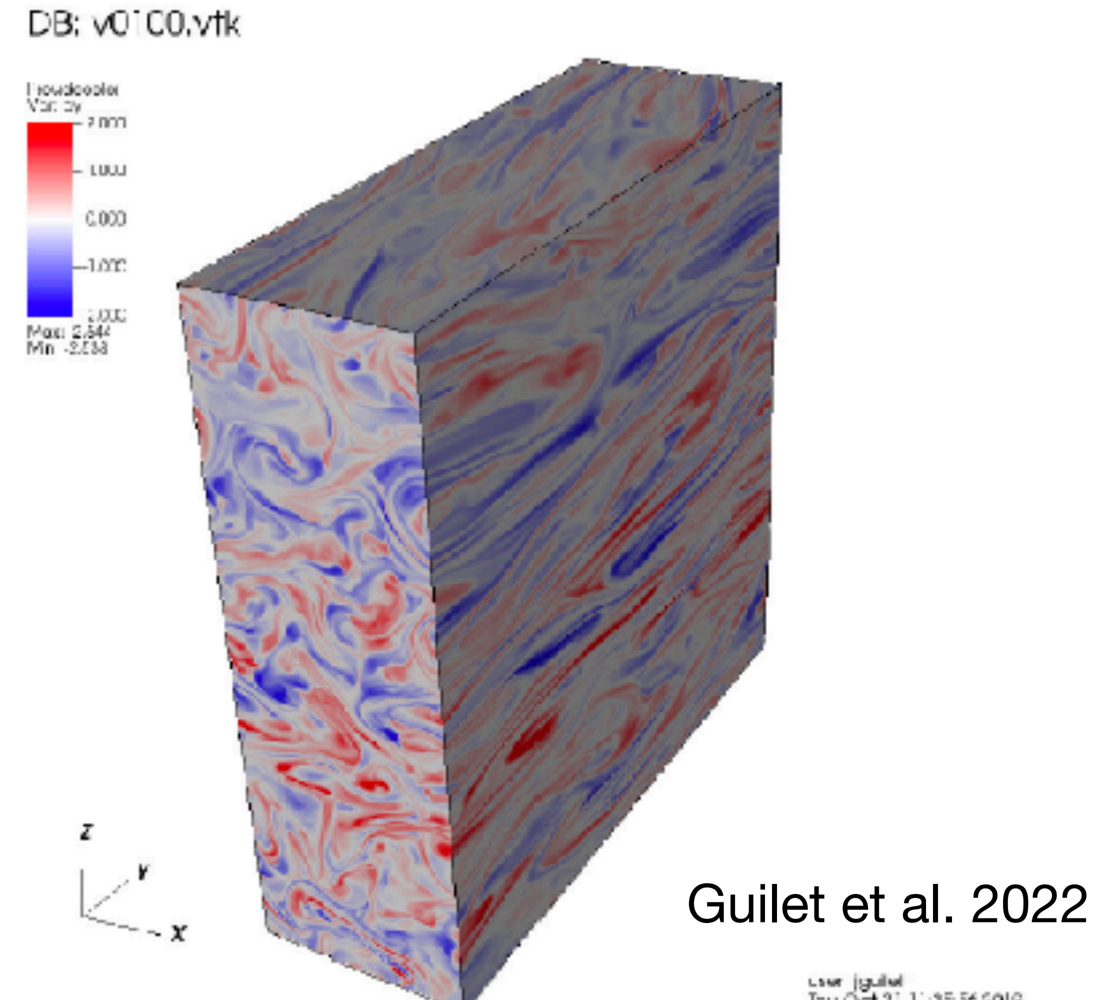

Guilet et al. 2022

Important parameters for HMNS (and PNS)

- Neutrino viscosity: Viscous impact on growth rate (Guilet+2015, 2017)
- High Magnetic Prandtl number Pm = viscosity/resistivity (Guilet+2022, Held+2022,+2024)
- Buoyancy: Brunt-Vaisala Frequency N/Ω (Guilet+2015)

Large-scale magnetic generation by the MRI

Mean-field approach

Mean field equations

$$\vec{B} = \overline{\vec{B}} + \vec{b} \quad \text{and} \quad \vec{U} = \overline{\vec{U}} + \vec{u}$$

Induction equation for mean field

$$\frac{\partial \overline{\vec{B}}}{\partial t} = \vec{\nabla} \times \left(\overline{\vec{U}} \times \overline{\vec{B}} + \vec{\mathcal{E}} - \eta \vec{\nabla} \times \overline{\vec{B}} \right)$$

with $\vec{\mathcal{E}} = \overline{\vec{u} \times \vec{b}}$

the electromotive force (EMF)

$$\mathcal{E}_i = \alpha_{ij} \overline{B}_j + \beta_{ij} \left(\vec{\nabla} \times \overline{\vec{B}} \right)_j + \ldots$$

Alpha effect $\quad \mathcal{E}_i = \alpha_{ij} \overline{B}_j$

$$t_{\alpha\Omega} = \frac{2\pi}{\sqrt{\alpha_{\phi\phi} \pi q \Omega / H}}$$

Gressel+2015, ARS+ 2022, Dhang+2024

alpha-Omega dynamo in PNS

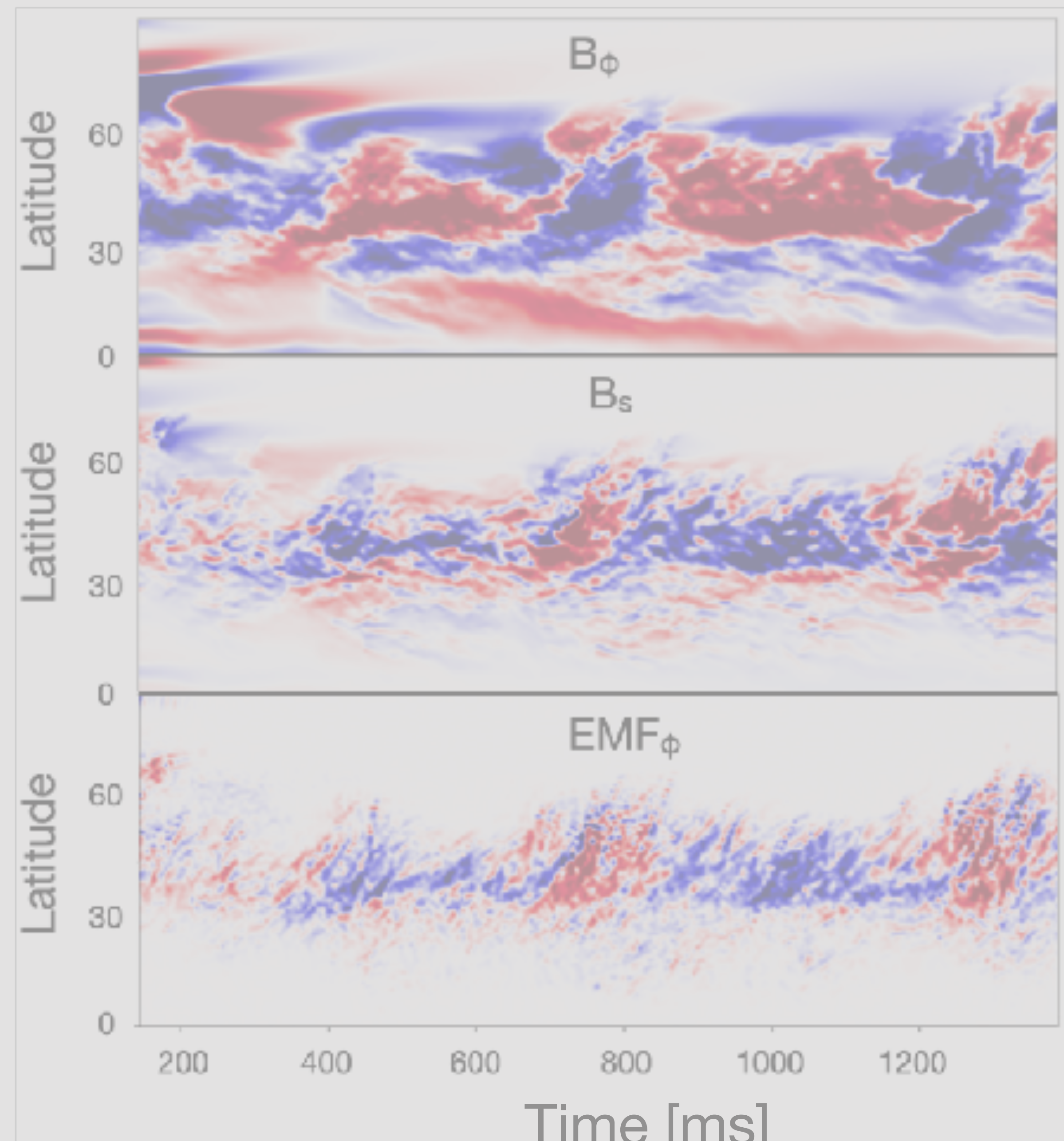

Reboul-Salze+2022

Setup for ideal 3D GRMHD simulations (Kiuchi, ARS, et al., 2024)

Numerical methods

- 3D ideal GRMHD radiation code in 3+1 formulation
- HLLD Riemann solver with CT-Contact (Kiuchi et al 2022)
- Static Mesh Refinement (16 levels)
- GR-Leakage + free-streaming neutrinos
- Equatorial plane symmetry
- Resolution $2N \times 2N \times N$ grid with $N = 361$
- Δx_finest = 12.5 m then relaxed to Δx = 50 m and Δx = 100 m

Initialisation

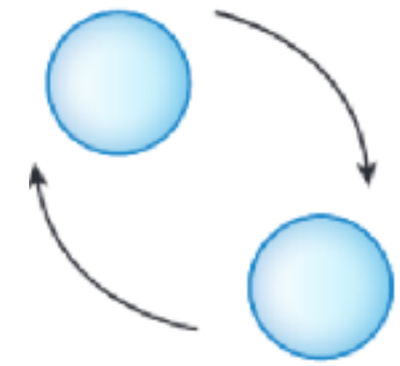

- $M_1 = M_2 = 1.35 M_\odot$ initialised with LORENE
- Irrotational neutron stars with initial orbital separation of ≈ 44 km
- DD2 equation of state Long-lived remnant for > O(1) s
- Initial vertical loop of $10^{15.5}$ G to reach realistic saturation energy of Kelvin-Helmholtz Instability and to resolve the MRI in the simulation
- We would require a resolution of Δx_finest < 7.5 m to start from a realistic seed field

Evolution of the simulation

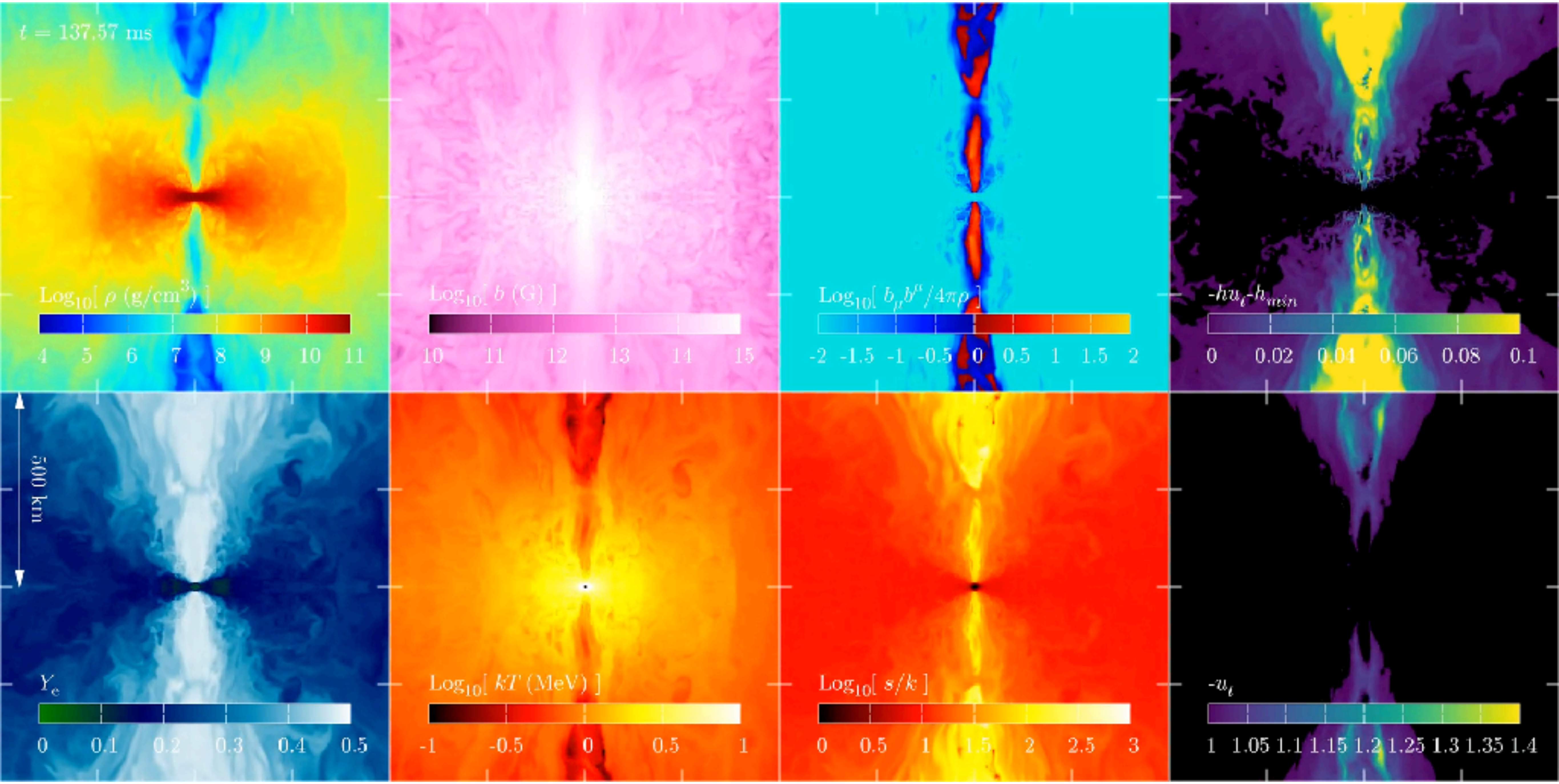

MRI-driven alpha-Omega dynamos in GRMHD simulations

Omega effect at R = 30 km

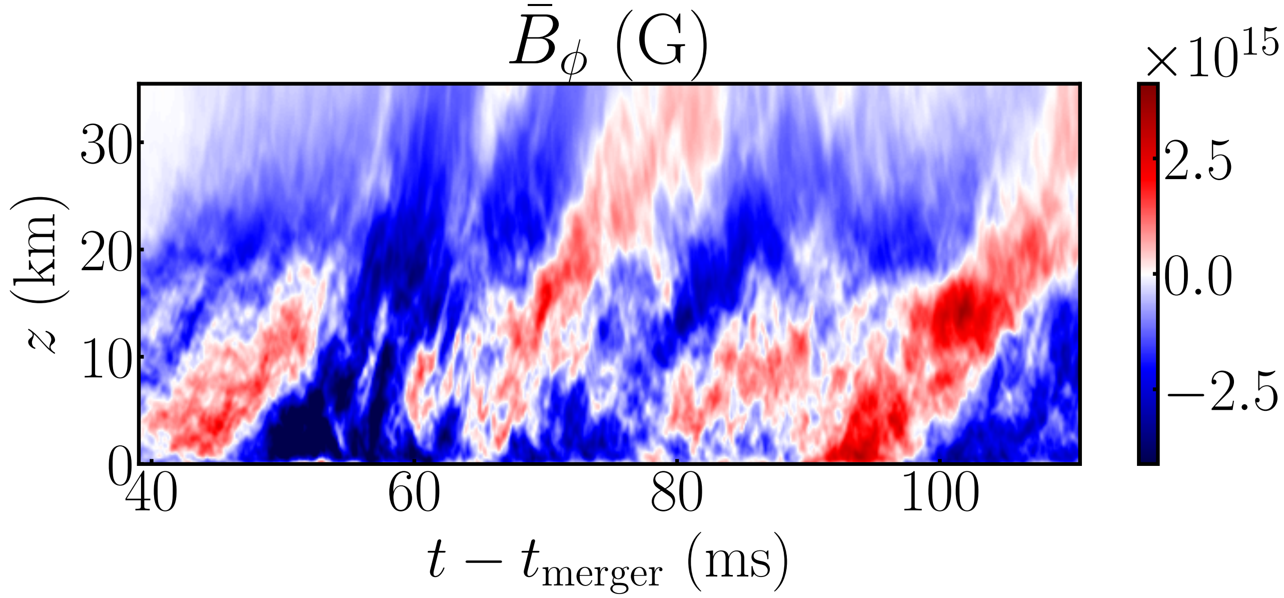

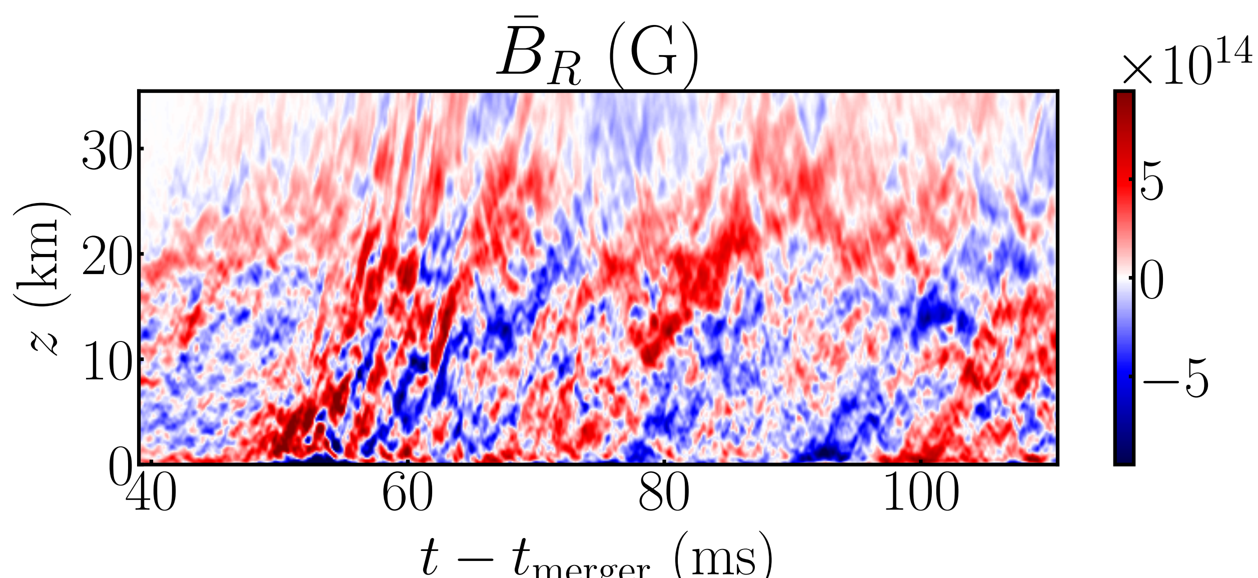

$$\frac{\partial \overline{B}_\phi}{\partial t} = \mathrm{R}\, \overline{B}_\mathrm{R} \frac{d\Omega}{ds}$$

alpha-effect at R = 30 km

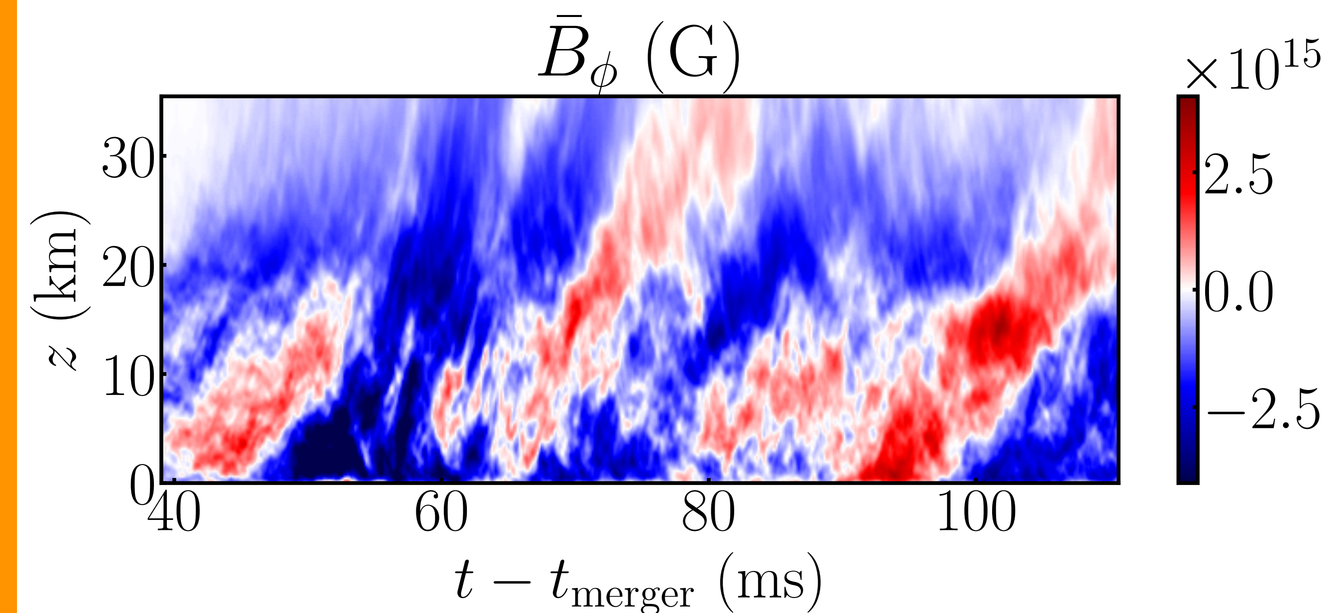

$$\vec{\mathcal{E}} = \overline{\vec{u} \times \vec{b}}$$

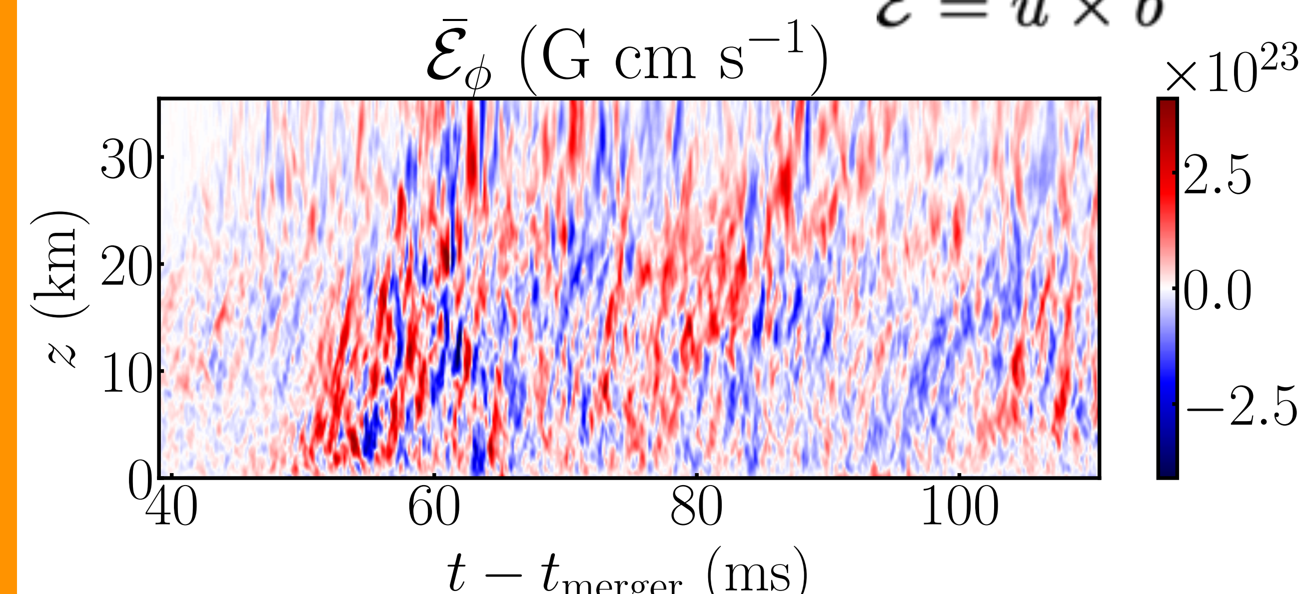

$$\mathcal{E}_\phi = \alpha_{\phi\phi} \bar{B}_\phi$$

Dynamo wave propagation

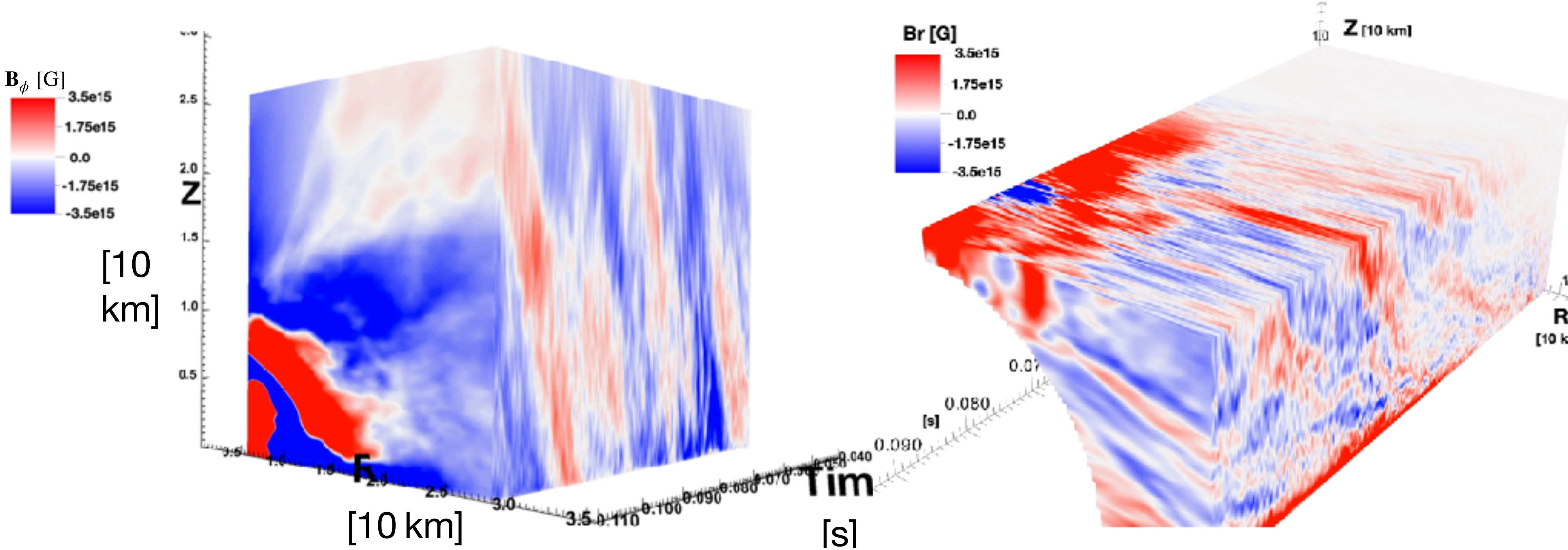

Magnetic field lines and jet

t= 144.8 ms

35 km

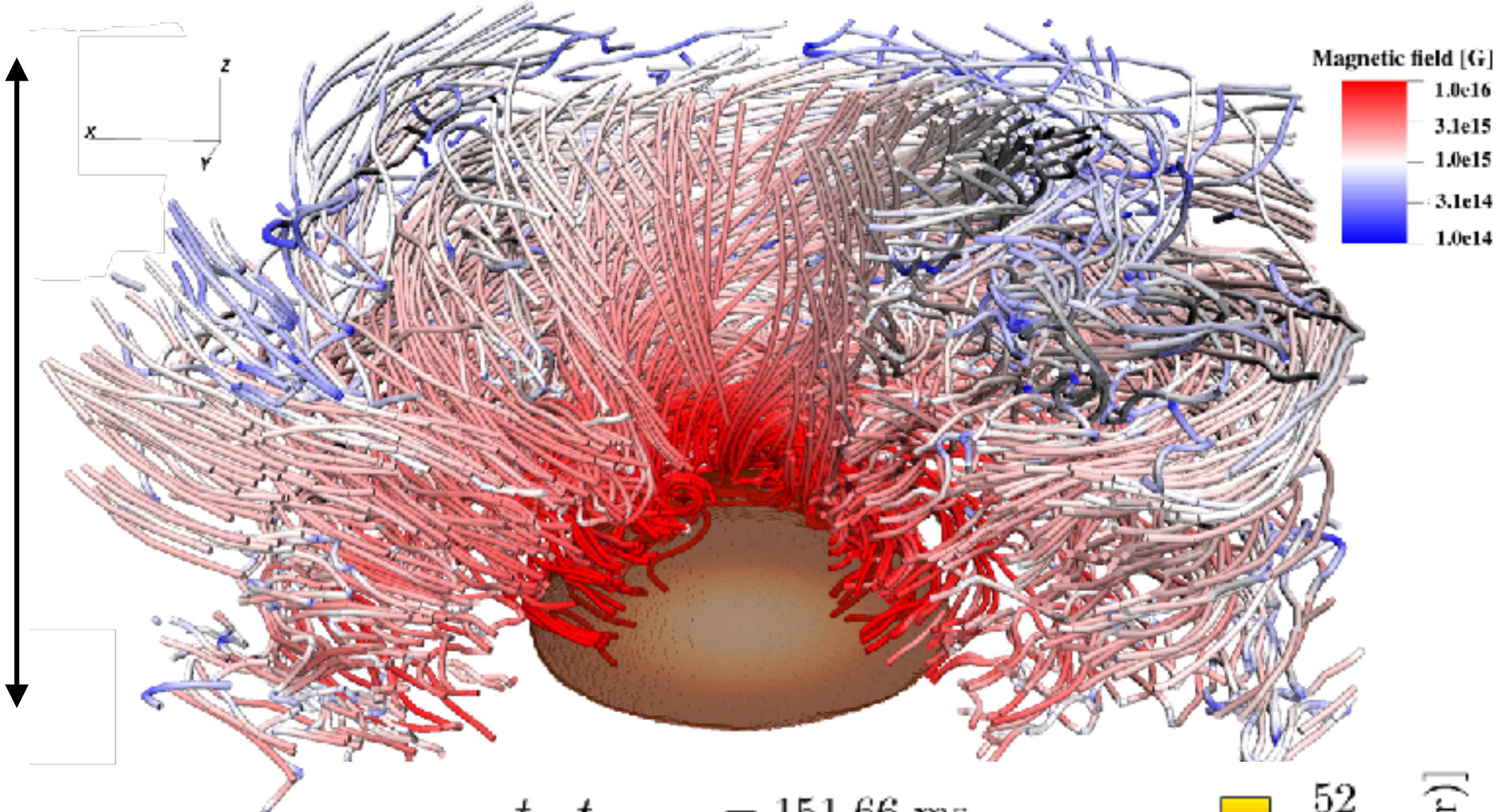

500 km

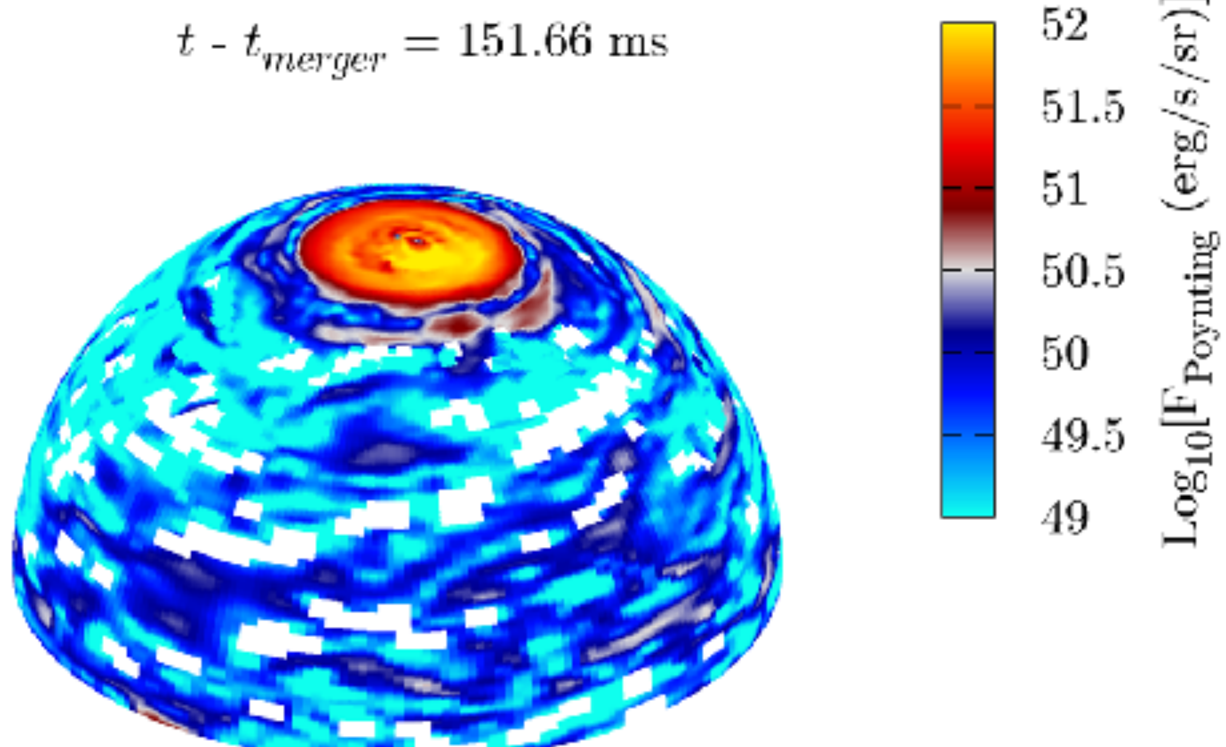

Turbulence dominated by the toroidal field

Jet starts from ~10 km

Pointing-flux isotropic luminosity
~ 10^{52} erg/s
Jet angle $\theta < 12^\circ$
Magnetisation parameter

$$\sigma_{LC} \equiv \frac{b^2}{4\pi\rho c^2} = 10 - 20$$

Luminosity time variability at 500 km comes from the dynamo period

Jet+winds:
Post-merger ejecta Mass
~ $0.1 M_\odot$

Microphysics: magnetic Prandtl number dependency

Pm regime in PNS and BNS merger

Magnetic Prandtl number: $Pm = \frac{\nu}{\eta}$

Diffusive approximation for neutrinos

Weak resistivity due to degenerate relativistic electrons

$Pm \sim 10^{13}$ $(Pm \sim 10^3 - 10^4)$

Guilet, ARS et al., 2022

Unstratified shearing box study with Snoopy

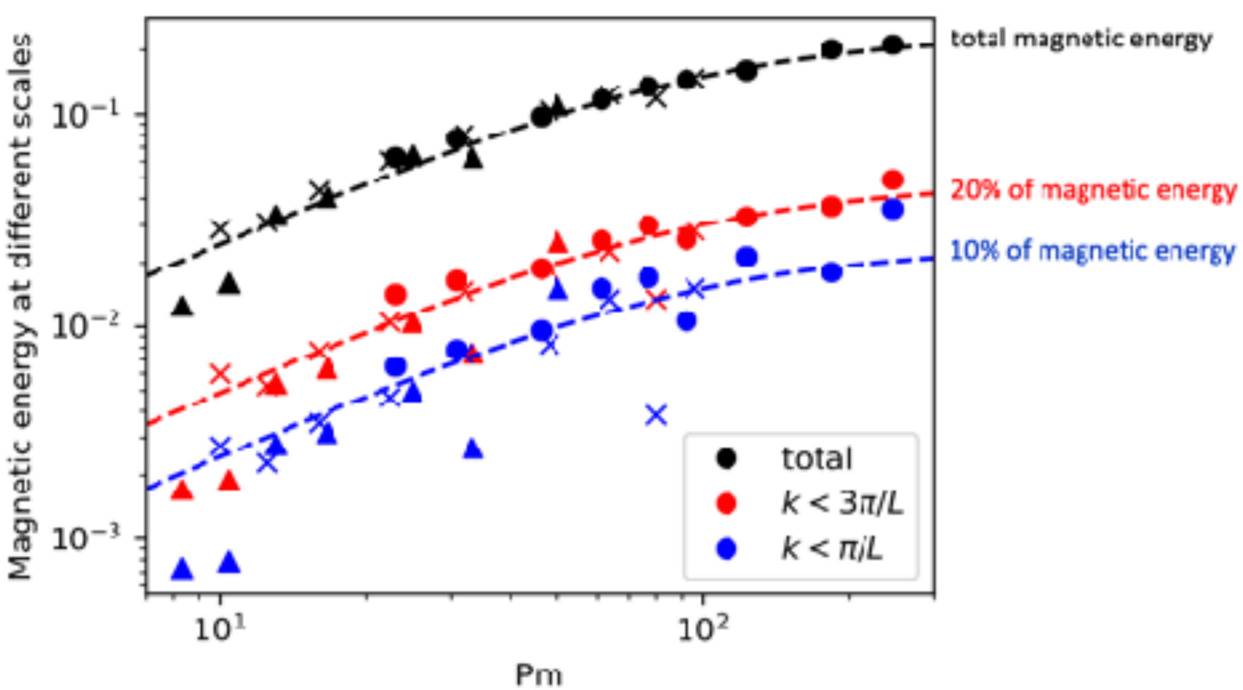

Held et al., 2024

Stratified case with increasing viscosity

Simulations made with PLUTO

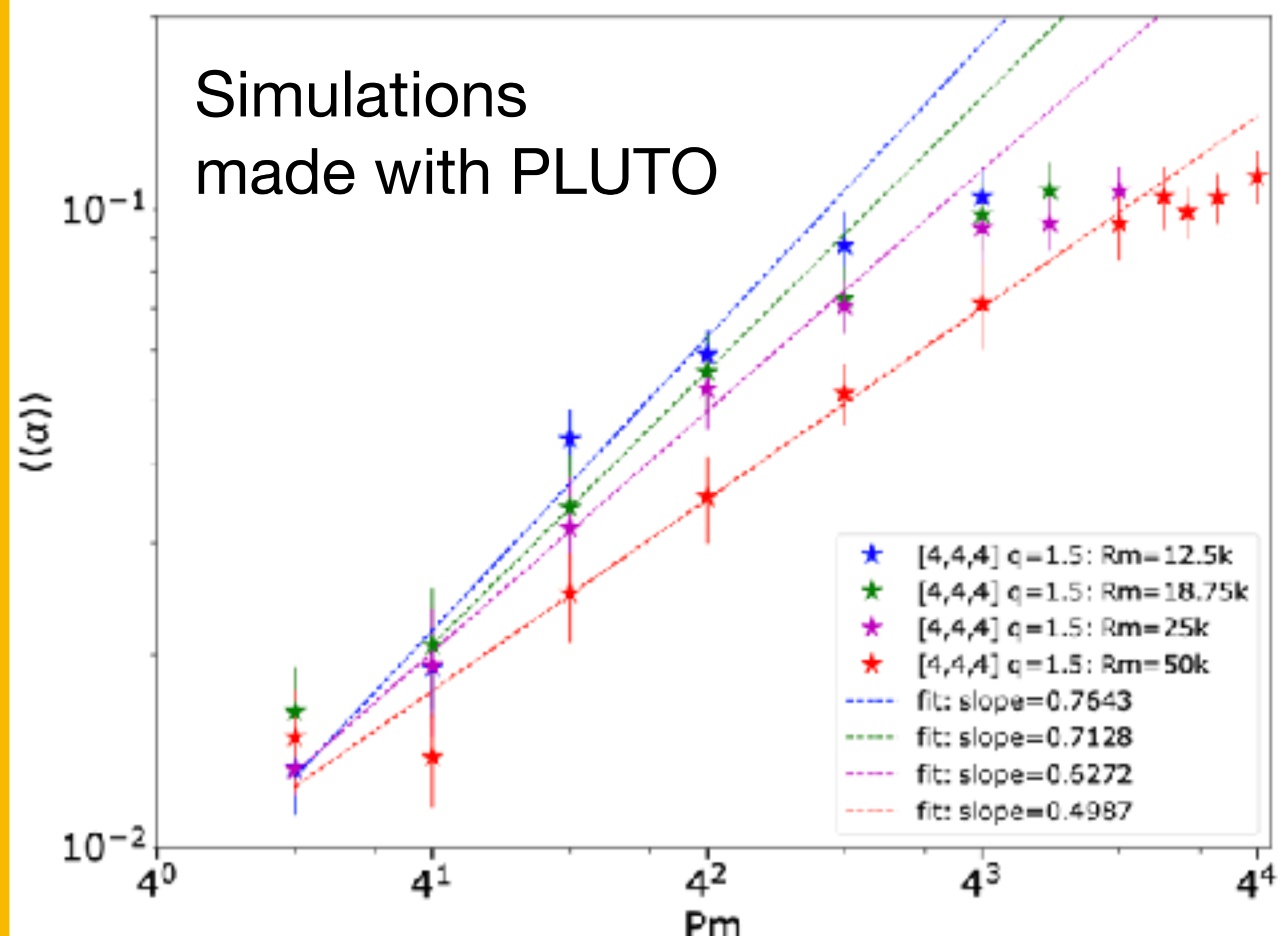

In the mid plane (|z|<2 H):
MRI-driven dynamo dynamics
In the "atmosphere" (|z|>2 H):
magnetic buoyancy instabilities

$H = \frac{c_s}{\Omega}$

Azimutal averaged magnetic field comparison

Pm=4 Pm=90

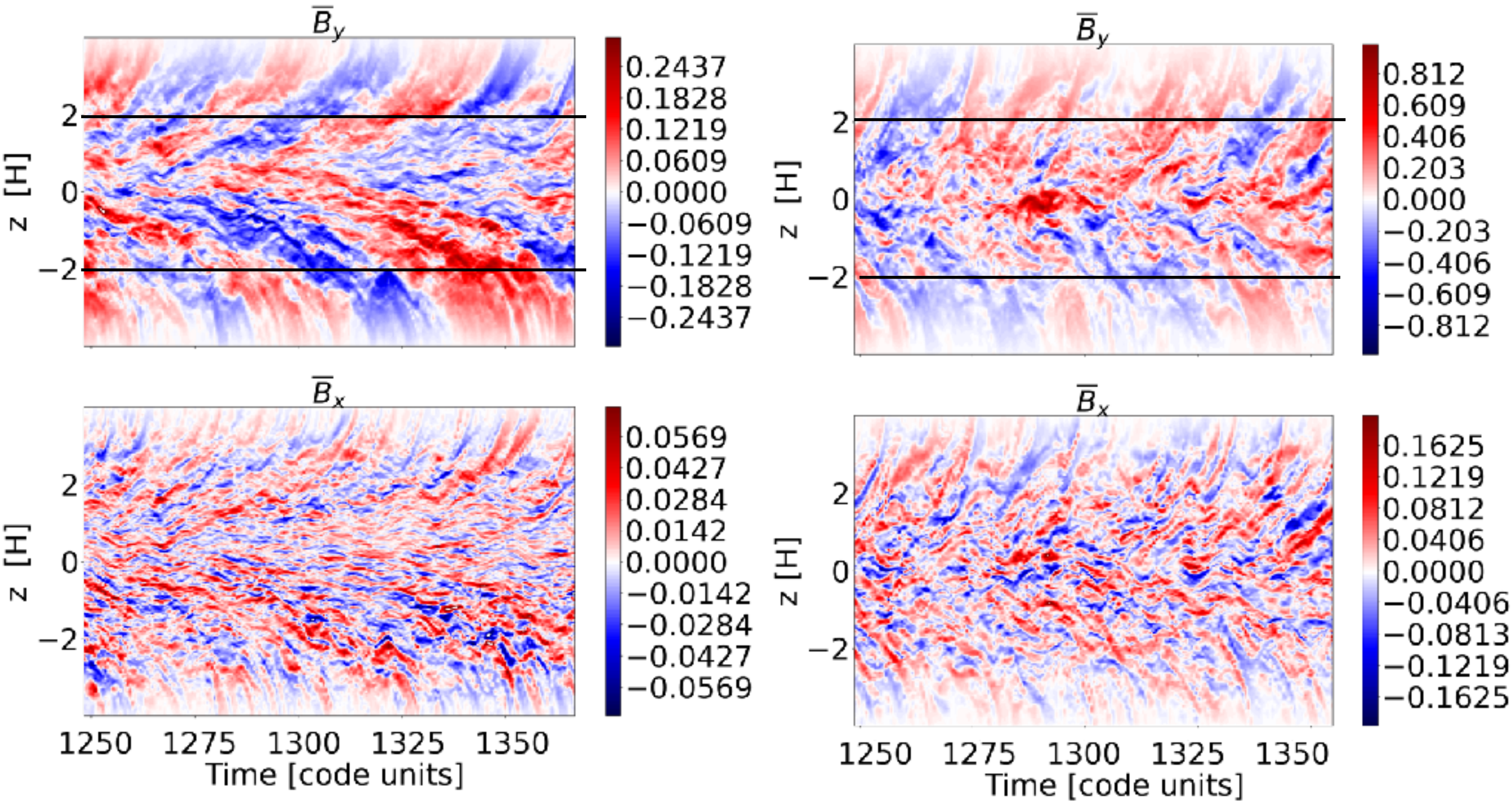

$P_{\alpha\Omega} \sim 10 - 11$ orbits ARS et al, 2025 $P_{\alpha\Omega} \sim 7 - 8$ orbits

Dynamo efficiency increased with Pm

Closure relation with turbulent pumping

$$\mathscr{E} = \alpha_{sym}\overline{B} + \vec{\gamma} \times \overline{B}$$

Dynamo terms can be computed one by one (Corr) or all terms at the same time (SVD, IROS)

Diagonal coefficient

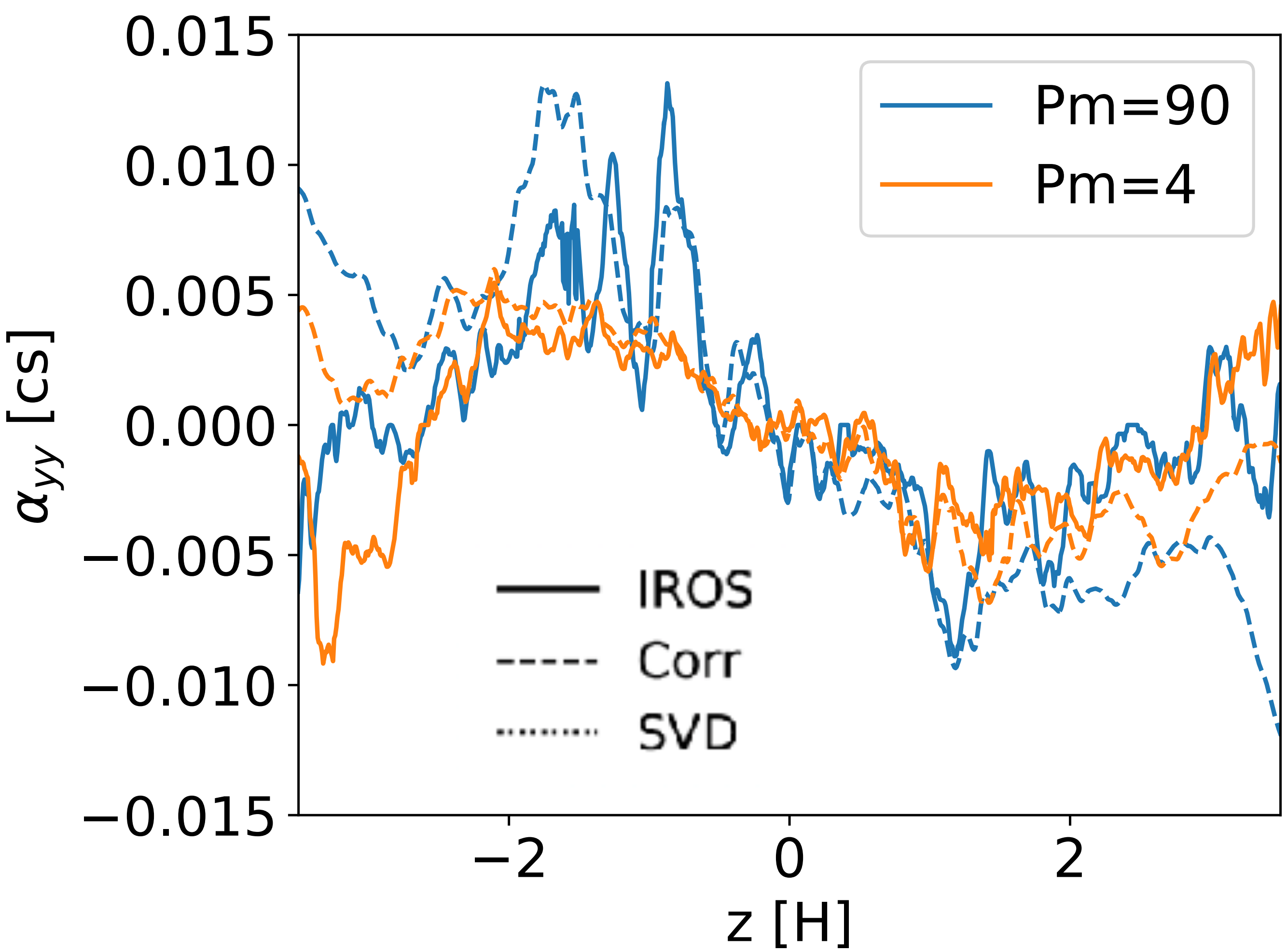

Starts to decrease out of the dynamo region

Vertical propagation

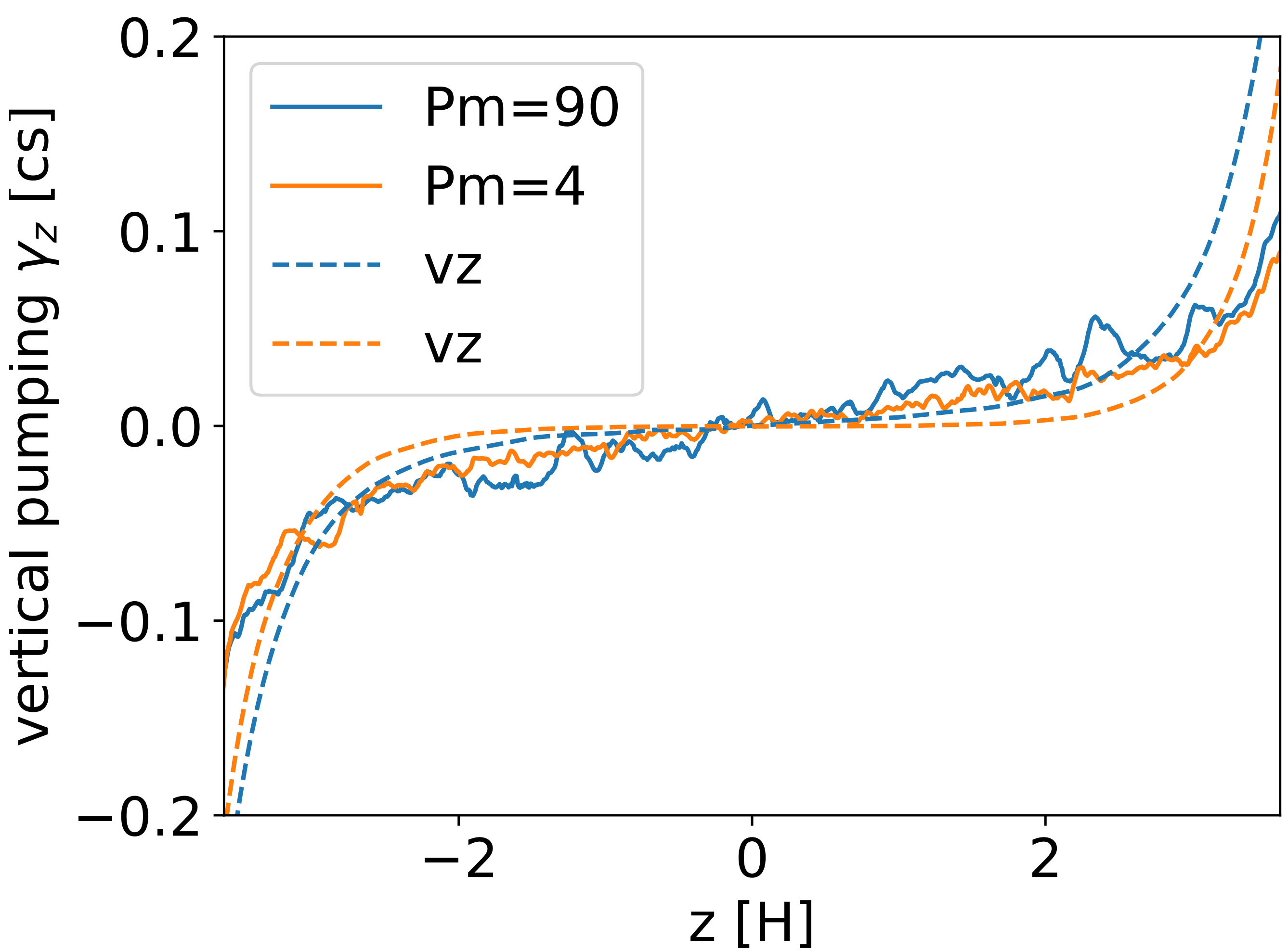

Propagation dominated
by turbulent pumping in dynamo region

Large-scale magnetic field amplification: global vs local

Peak alpha strength

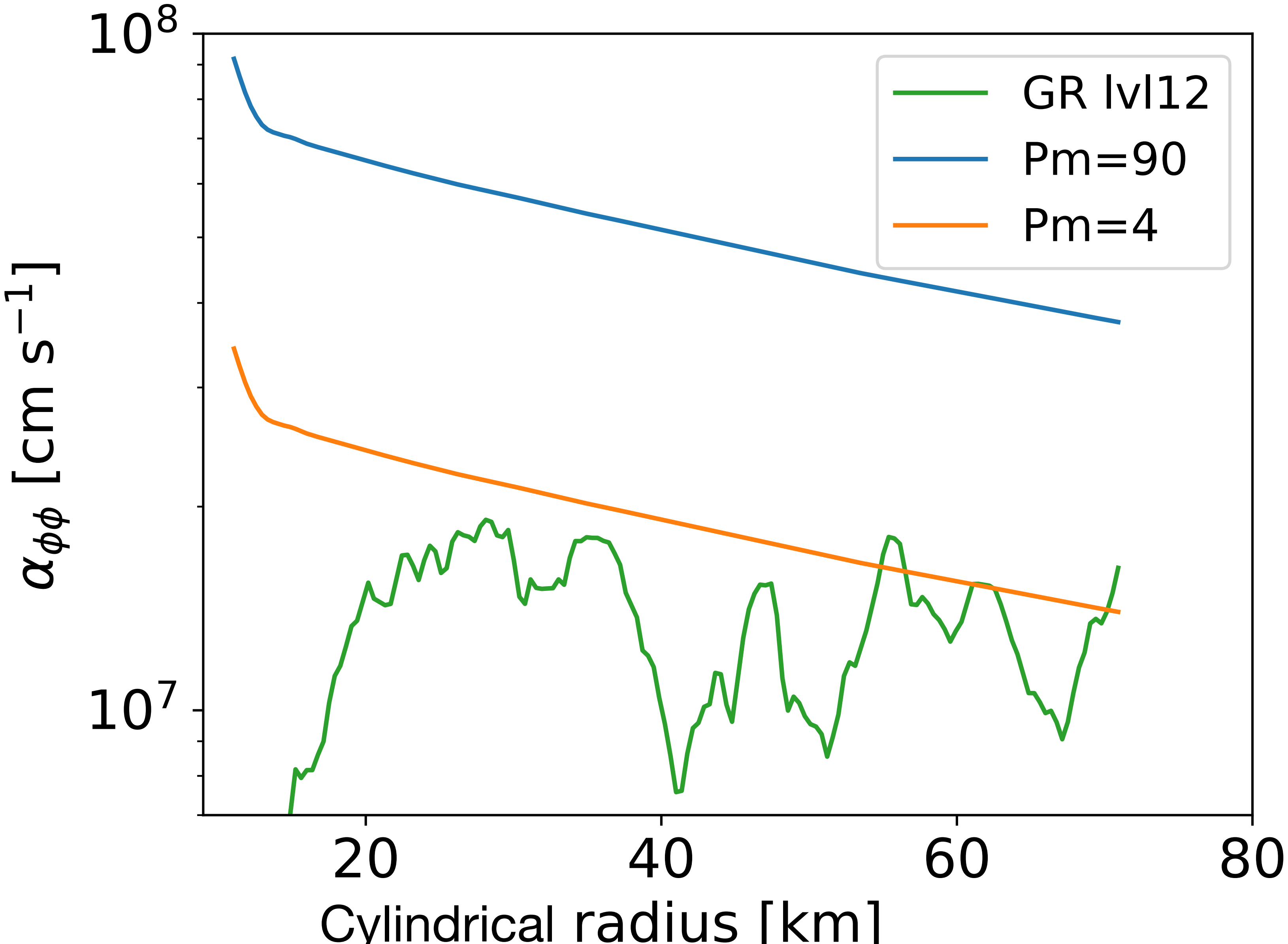

ARS et al, 2025

Comparison with GRMHD simulation
(Kiuchi et al. 2024)

- Faster growth rate and period

$$P = 2\pi \left(\frac{1}{2} \alpha_{\phi\phi} \frac{d\Omega}{d \ln s} k_z \right)^{-1/2}$$

~ 14-18 ms instead of 20-25 ms

- Magnetic field would be > 3-5 times higher than GRMHD simulation

- Faster Propagation (off-diagonal alpha component)

- Stronger winds + more luminous jets compared to GRMHD simulations

Summary and Perspectives

- MRI-driven alpha-Omega dynamo in BNS mergers

⟶ Self-consistent MRI-driven alpha-Omega dynamo with ~20 ms period
⟶ Launch of a relativistic collimated outflow with high luminosity
⟶ Dynamo period impacts the variability in the jet luminosity
⟶ How the period changes with NS masses, EOS?
⟶ In case of collapse to a BH -> jet power, dynamo period?

- High-Pm regime: higher dynamo efficiency

⟶ Faster growth rate, variability and propagation
⟶ More luminous and magnetised jets
⟶ Stronger winds of the HMNS and disks
⟶ **Explore this regime with 2D axisymmetric simulations with dynamo terms/ subgrid modelling?**

Global BNS merger setup

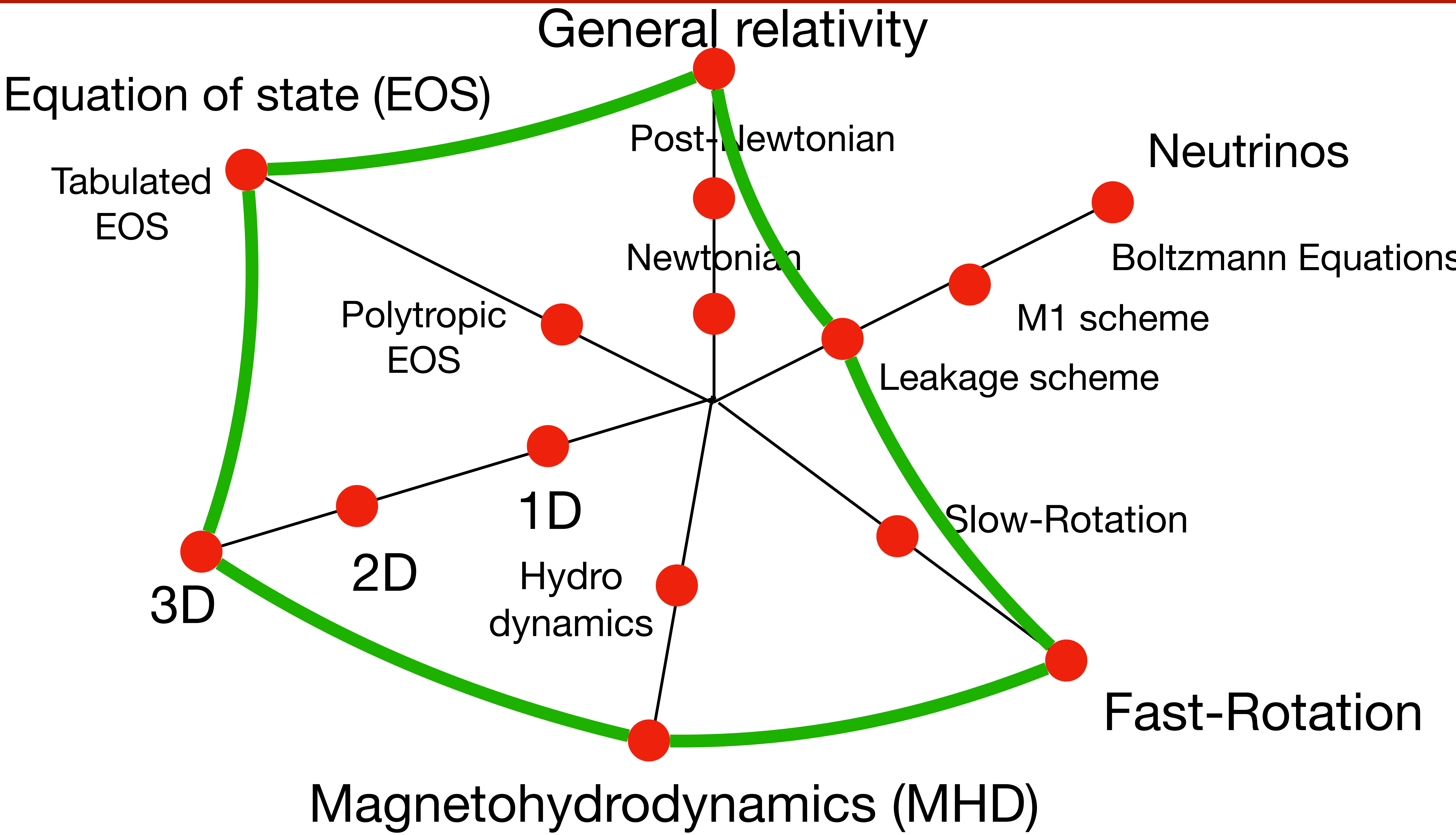

Impact on the GRB luminosity?

FFT of toroidal field at 12 km in the HMNS

Poynting Flux luminosity at 500 km

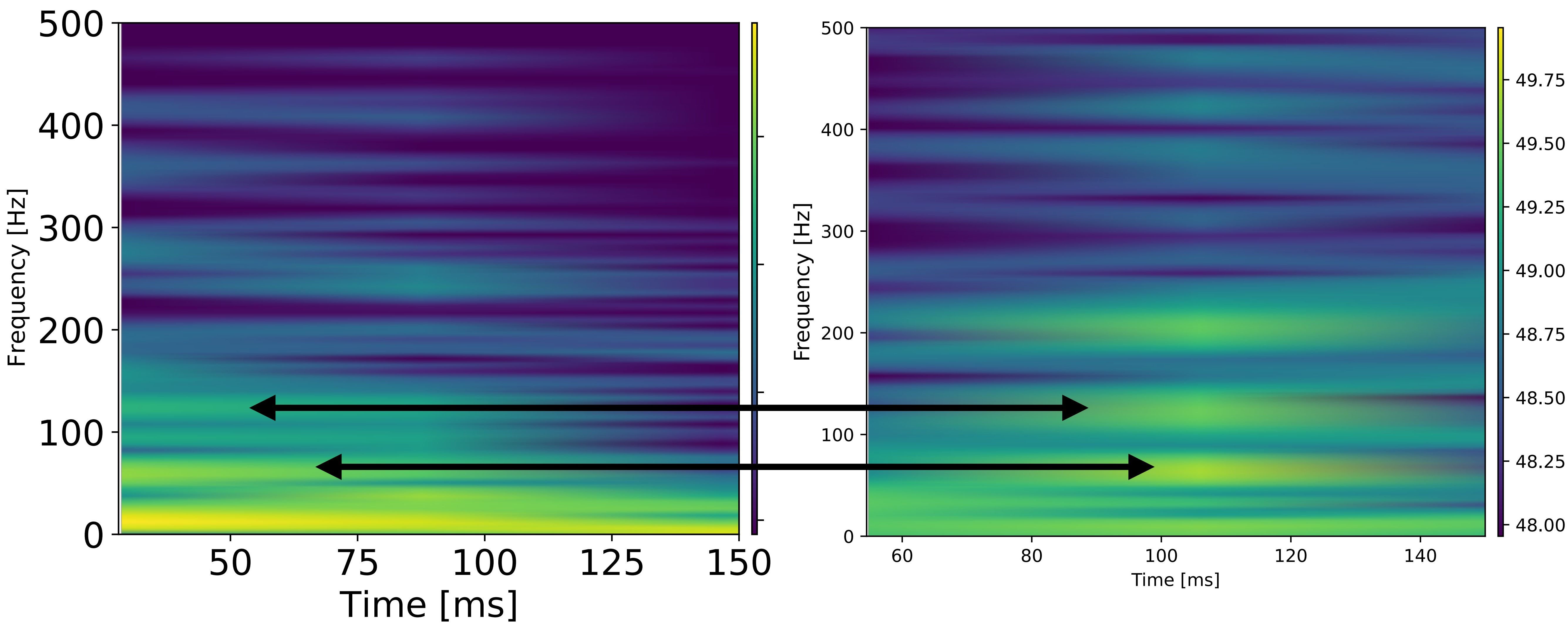

Reboul-Salze et al, in prep

How does this variability evolves with the jet propagation?

Some GRBs observations have some low-frequency quasi-periodic oscillations: around 20, 40, 60 Hz for GRB 181222B (Caballero-Garcia et al. 2025)

How does the dynamo frequency changes with initial conditions, EOS and microphysics?

Mean-field theory

Principle

$$\vec{B} = \overline{\vec{B}} + \vec{b} \quad \text{et} \quad \vec{U} = \overline{\vec{U}} + \vec{u}$$

Induction equation for mean field

in ideal GRMHD

$$\frac{\partial \overline{\vec{B}}}{\partial t} = \vec{\nabla} \times \left(\overline{\vec{U}} \times \overline{\vec{B}} + \vec{\mathcal{E}} - \eta \vec{\nabla} \cancel{\times \overline{\vec{B}}} \right)$$

with $\vec{\mathcal{E}} = \overline{\vec{u} \times \vec{b}}$ the electromotive force (EMF)

Dynamo loop

Omega effect $\quad \dfrac{\partial B_\phi}{\partial t} = r \sin\theta \vec{B}_P \cdot \vec{\nabla}\Omega$

Alpha effect $\quad \mathcal{E}_i = \alpha_{ij} \overline{B}_j$

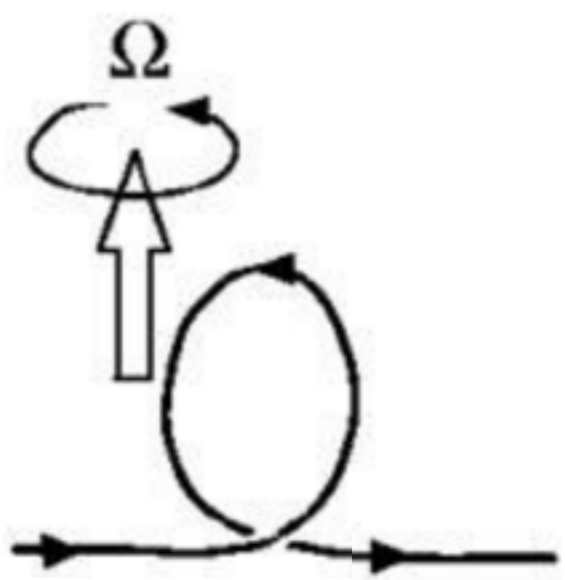

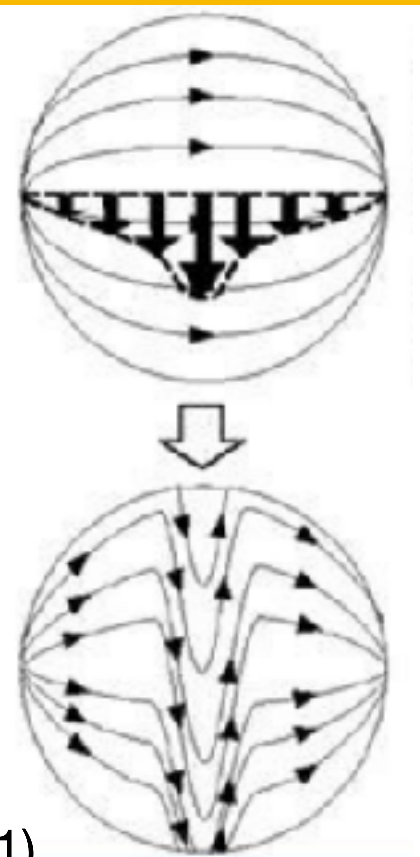

How to compute the coefficients:

$$\alpha_{ij} = \frac{\langle \mathcal{E}_i \overline{B}_j \rangle}{\langle \overline{B}_j^2 \rangle}.$$

- → correlation estimations
- → Matrix estimation: Singular value decomposition (SVD) (Racine+2011)

Methods to estimate the dynamo coefficient

Simple fit method

Hypotheses: Only one contribution dominates each EMF component

~ Valid if high correlation

⟶ Alpha tensor

$$\alpha_{ij} = \frac{\langle \mathcal{E}_i \overline{B}_j \rangle}{\langle \overline{B}_j^2 \rangle}.$$

IROS Method

Algorithm to remove sources iteratively

1. **Initialization:** Start with zero values for α_{ij} and β_{ij}.
2. **Fitting:** At each spatial position, fit the EMF time series against **B** and **J** to extract first-order estimates.
3. **Refinement:** Iteratively subtract a percentage of the best-fit contributions from the EMF and update coefficients until convergence.

Best performance from tests

Dhang et al. 2024

SVD decomposition

EMF
$$\mathcal{Y} = \begin{pmatrix} \bar{\mathcal{E}}_r(t_1) & \bar{\mathcal{E}}_\theta(t_1) & \bar{\mathcal{E}}_\phi(t_1) \\ \bar{\mathcal{E}}_r(t_2) & \bar{\mathcal{E}}_\theta(t_2) & \bar{\mathcal{E}}_\phi(t_2) \\ \vdots & \vdots & \vdots \\ \bar{\mathcal{E}}_r(t_N) & \bar{\mathcal{E}}_\theta(t_N) & \bar{\mathcal{E}}_\phi(t_N) \end{pmatrix},$$

B field
$$\mathcal{A} = \begin{pmatrix} \bar{B}_r(t_1) & \bar{B}_\theta(t_1) & \bar{B}_\phi(t_1) \\ \bar{B}_r(t_2) & \bar{B}_\theta(t_2) & \bar{B}_\phi(t_2) \\ \vdots & \vdots & \vdots \\ \bar{B}_r(t_N) & \bar{B}_\theta(t_N) & \bar{B}_\phi(t_N) \end{pmatrix}.$$

$$\mathcal{Y}(r,\theta) = \mathcal{A}(r,\theta)\,\mathcal{X}(r,\theta) + \mathcal{N}(r,\theta)$$ Noise

Unique decomposition of matrix A :

$$\mathcal{A} = \mathbf{U}\mathbf{w}\mathbf{V}^T$$

where w is a diagonal 3x3 matrix,
U a N x 3 matrix, and V a 3x3 matrix.

alpha tensor is then given then by

$$\hat{\boldsymbol{x}}_j = \mathbf{V}\mathbf{w}^{-1}\mathbf{U}^T\boldsymbol{y}_j$$

Advantages : Full alpha tensor

Racine et al 2011, Dhang et al. 2020

alpha effect

Pm=4

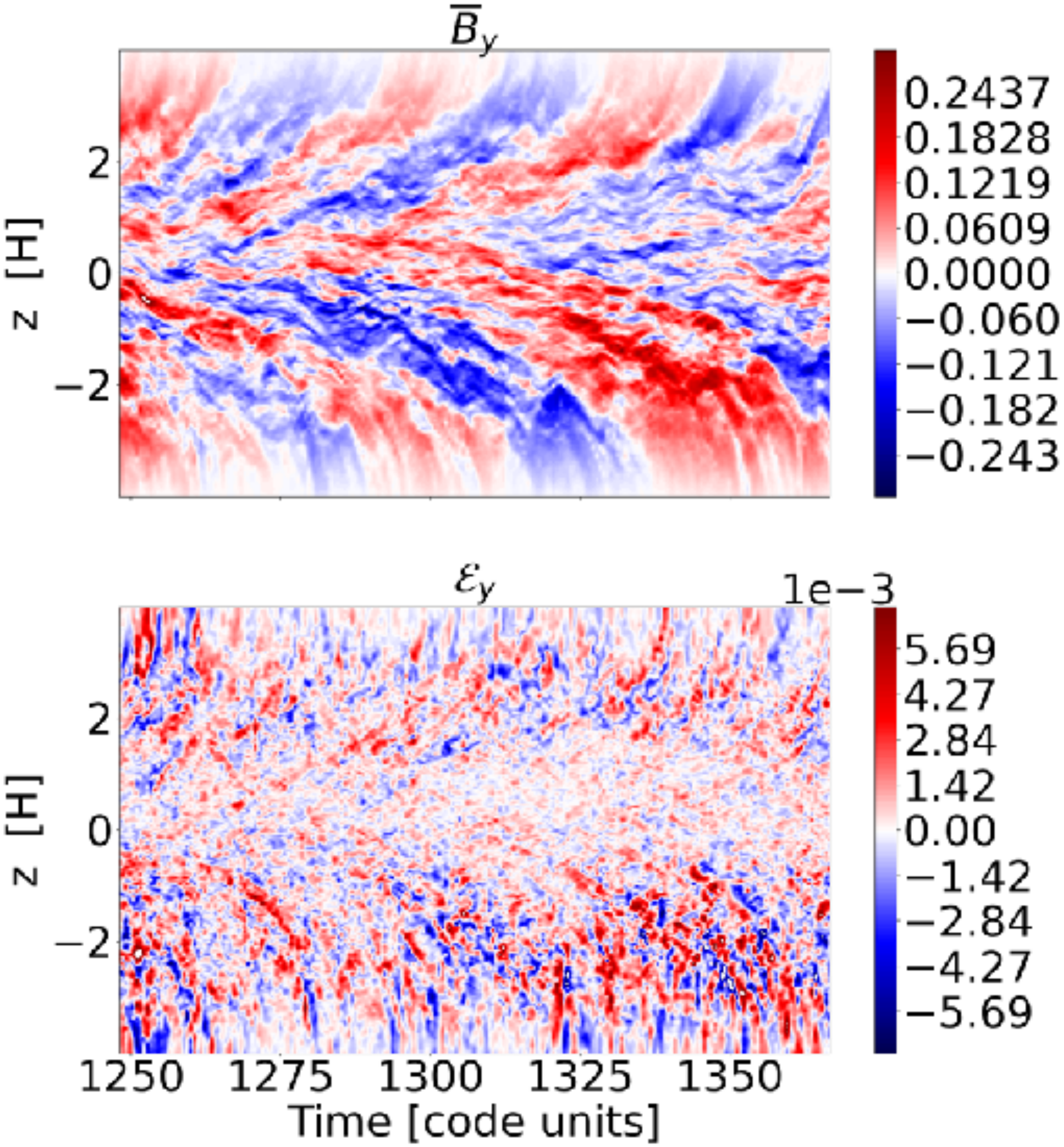

$$\mathcal{E}_\phi = \alpha_{\phi\phi}\bar{B}_\phi$$

Pm=90

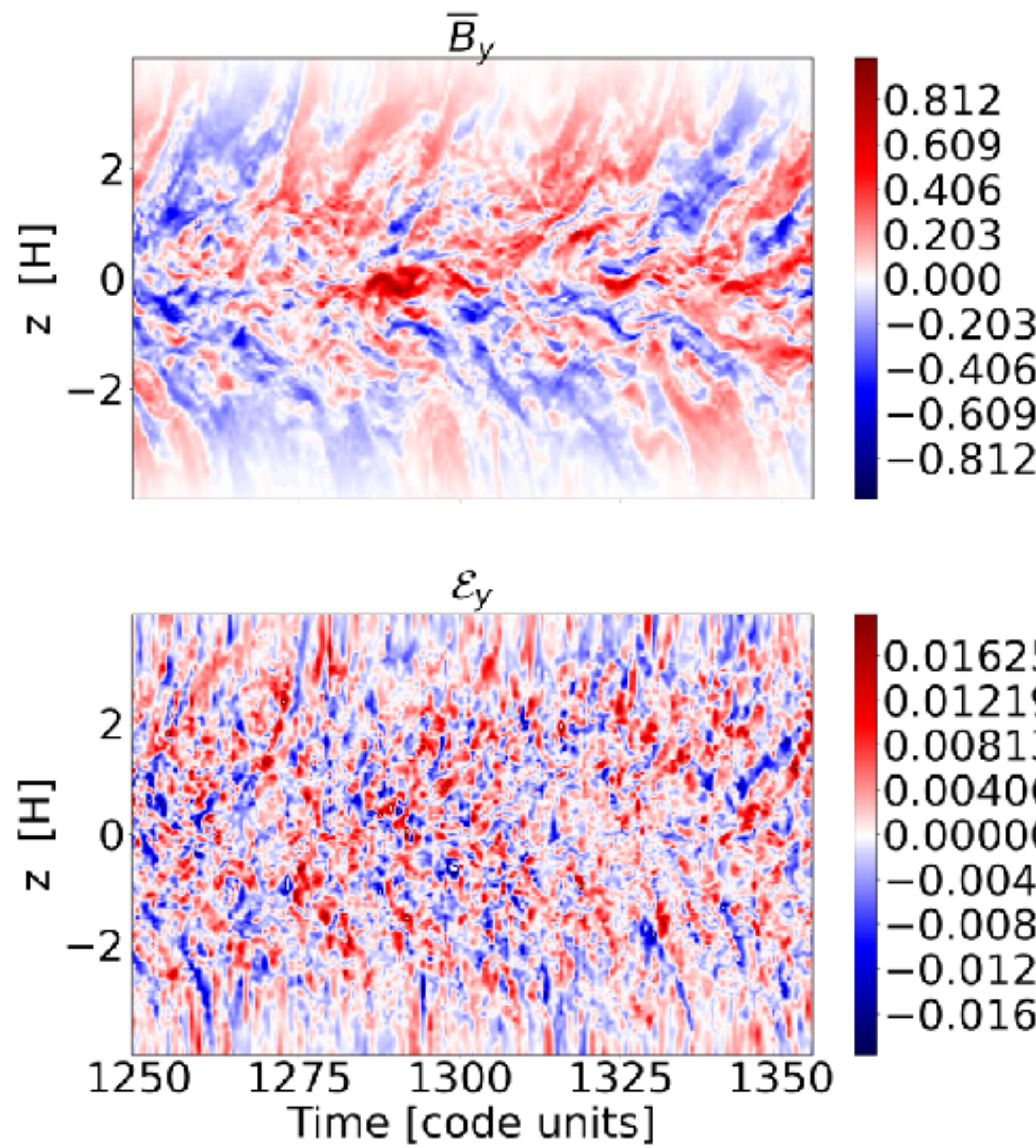

$$\mathcal{E}_\phi = \alpha_{\phi\phi}\bar{B}_\phi$$

Time evolution of the MRI-unstable zone

Energy evolution when $\rho < 10^{14.5}$ g cm^{-3}